



## Thermal contraction crack polygons on Mars: Classification, distribution, and climate implications from HiRISE observations

Joseph Levy,<sup>1</sup> James Head,<sup>1</sup> and David Marchant<sup>2</sup>

Received 29 September 2008; revised 2 November 2008; accepted 14 November 2008; published 28 January 2009.

[1] Documenting the morphology and distribution of polygonally patterned ground on Mars is critical for understanding the age and origin of the Martian latitude-dependent mantle. Polygonally patterned ground on Mars is analyzed using High Resolution Imaging Science Experiment image data in order to document the variation of polygon morphology within latitude bands 30–80° in both northern and southern hemispheres. Small-scale (<~25 m diameter) polygons are classified on the basis of morphological characteristics into seven groups, which are present in both northern and southern hemispheres. Polygon morphology is shown to be consistent with thermal contraction cracking of an ice-rich mantling unit, consistent with observations of sediment wedge thermal contraction crack polygons forming in ice-cemented sediment at the Phoenix landing site. Polygon groups are distributed symmetrically in both northern and southern hemispheres, suggesting strong climate controls on polygon morphology. Northern hemisphere polygonally patterned surfaces are found to decrease in age from low to high latitude, spanning surface ages from ~1 to <0.1 Ma, suggesting more recent deposition of ice-rich material at high latitudes than at low latitudes. Six of the seven classes of polygons are interpreted to be capable of forming because of the combined effects of thermal contraction cracking and differential sublimation, suggesting that sublimation and sand wedge polygons dominate Martian high latitudes. Gully polygon systems present at midlatitudes suggest that small amounts of liquid water may have been involved in thermal contraction crack polygon processes, producing composite wedge polygons. No evidence is found for the presence of pervasive small-scale ice wedge polygons.

**Citation:** Levy, J., J. Head, and D. Marchant (2009), Thermal contraction crack polygons on Mars: Classification, distribution, and climate implications from HiRISE observations, *J. Geophys. Res.*, 114, E01007, doi:10.1029/2008JE003273.

### 1. Introduction

[2] Polygonally patterned ground on Mars has been explored and characterized by orbiting and landed spacecraft for more than 30 years [Mutch *et al.*, 1976; Lucchitta, 1981; Mangold, 2005; Smith *et al.*, 2007; Mellon *et al.*, 2008], and has been used to infer the presence of [Malin and Edgett, 2001; Mangold *et al.*, 2004; Mangold, 2005] and directly analyze [Smith, 2008] ice-rich permafrost. Thermal contraction cracking of an ice-rich substrate, such as the latitude-dependent mantle considered here, has been shown to be a plausible mechanism for generating trough-bounded polygons at Martian latitudes poleward of ~30° under current climate conditions [Mellon, 1997; Mellon *et al.*, 2008]. Understanding the origin and history of Martian subsurface ice reservoirs: deconvolving primary atmospheric deposition that forms massive ice deposits, from cyclical vapor diffusion, that generates pore-ice deposits remains an active area

of inquiry [Mustard *et al.*, 2001; Head *et al.*, 2003; Schorghofer and Aharonson, 2005; Kostama *et al.*, 2006; Schorghofer, 2007]. Particular attention has been focused on understanding the ages (~0.1 Ma [Kostama *et al.*, 2006] to ~1 Ma [Mangold, 2005]), deposition/modification histories [Kostama *et al.*, 2006; Kreslavsky *et al.*, 2008; Schorghofer, 2007], and morphological expressions [Mangold, 2005] of Martian polygonally patterned ground, and by extension, the age and nature of Martian latitude-dependent mantle deposits [Mustard *et al.*, 2001; Head *et al.*, 2003].

[3] Analyses of polygonally patterned ground at Viking, THEMIS, and MOC resolutions leave several significant issues outstanding: to what extent is liquid water involved in Martian polygon development [Mangold, 2005]; does thermal contraction cracking account for the complete range of polygonally patterned ground observed on Mars [Mangold, 2005]; how do the ages of different polygonally patterned units vary [Mangold, 2005; Kostama *et al.*, 2006]; and how does polygonally patterned ground fit into broader-scale ice-related activity during the late Amazonian [Mustard *et al.*, 2001; Head *et al.*, 2003; Milliken *et al.*, 2003]?

[4] The High Resolution Imaging Science Experiment (HiRISE) [McEwen *et al.*, 2007] is uniquely well suited to address these issues. HiRISE image data permit analysis of polygonally patterned ground at resolutions equal to or

<sup>1</sup>Department of Geological Sciences, Brown University, Providence, Rhode Island, USA.

<sup>2</sup>Department of Earth Sciences, Boston University, Boston, Massachusetts, USA.

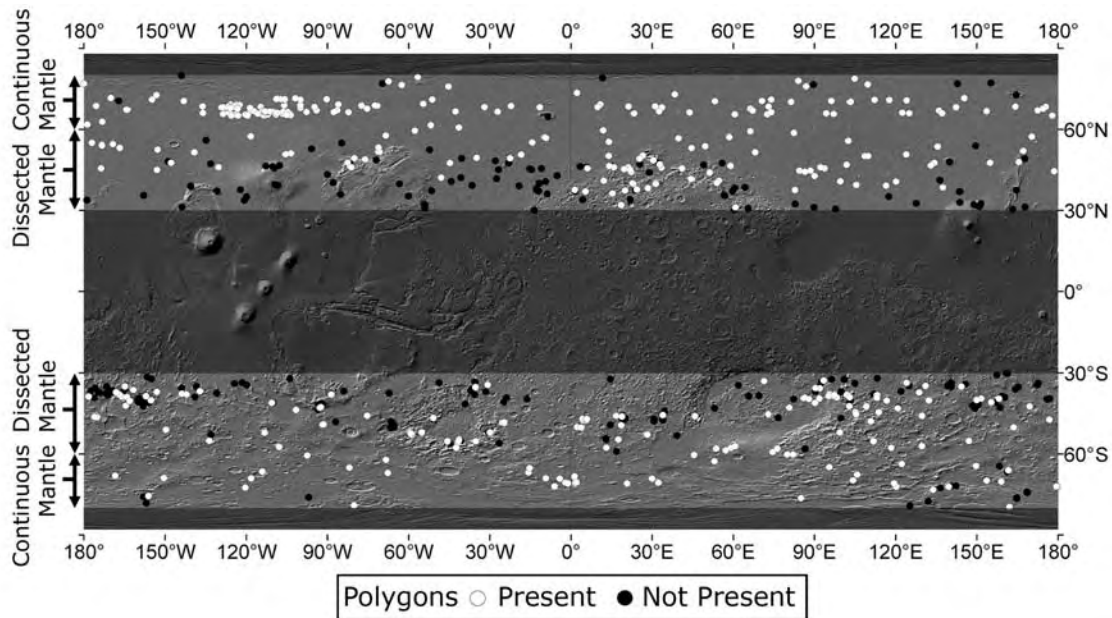


**Figure 1.** Distribution map of HiRISE images in which features interpreted to be thermal contraction crack polygons are (white circles) and are not (black circles) present. There were 823 images analyzed in this study; 276 images contain polygons in the northern hemisphere and 207 images contain polygons in the southern hemisphere. Highlighted regions show latitude range of image survey. Continuous and dissected mantle indicate the range of continuous and dissected latitude-dependent mantle surfaces, respectively, mapped by *Milliken et al.* [2003]. Base map is Mars Orbiter Laser Altimeter shaded relief.

exceeding the resolution of terrestrial air photographs [Black, 1952]. This analysis of HiRISE primary science phase (PSP) images was conducted in order to answer the following questions. (1) How does the morphology of polygonally patterned ground vary across the Martian surface at HiRISE resolution? (2) What does variation in polygon morphology indicate about the latitude-dependent mantle in which polygons have formed? (3) What does variation in polygon morphology indicate about the climate conditions (including temperature and water activity) under which the polygons developed? (4) What is the formational history, age, and stratigraphy of polygonally patterned units on Mars, and how does this correlate with orbital forcing and broad-scale glacial processes? Answers to these questions would provide a context in which to interpret ground observations from the Phoenix lander, and would inform understanding of potentially habitable Martian permafrost environments.

## 2. Survey Parameters

[5] A total of 823 full-resolution HiRISE images (413 northern hemisphere, 410 southern hemisphere), spanning primary science phase (PSP) orbits 001330–006981 [McEwen *et al.*, 2007], form the basis for this survey (Figure 1). Most images have a processed resolution of  $\sim 30$  cm/pixel, however some were resampled to  $\sim 50$  cm/pixel prior to downlink [McEwen *et al.*, 2007]. For comparison, a typical  $\sim 1$  GB HiRISE image contains approximately 200 times more information than a typical 5MB Mars Orbiter Camera image, resulting from increased spatial resolution within a comparable surface footprint.

[6] From the complete set of publicly released HiRISE images, a subset was selected for detailed analysis. All

analyzed images are located between latitudes  $30\text{--}80^\circ$ . These latitude bands were selected because (1) poleward of  $\sim 25\text{--}30^\circ$ , thermal contraction stresses are found to be sufficient to produce failure of ice-cemented sediments (stress  $> \sim 2$  MPa) under current surface conditions [Mellon, 1997]; (2) abundant examples of polygonally patterned ground have been observed in these regions using other image data sets [Mangold, 2005]; (3) these latitudes span continuous and dissected latitude-dependent mantle surfaces, which are interpreted to record the deposition of recent Amazonian, ice-rich sediments [Kreslavsky and Head, 1999; Mustard *et al.*, 2001; Head *et al.*, 2003; Milliken *et al.*, 2003]; (4) inferred hydrogen abundance maps indicate abundant water-ice within  $\sim 80$  cm of the surface in a subset of these latitudes [Boynton *et al.*, 2002; Feldman *et al.*, 2002; Kuzmin *et al.*, 2004; Mitrofanov *et al.*, 2007]; and (5) poleward of  $80^\circ$  latitude, polar cap processes dominate.

[7] After selecting images on the basis of latitude, images spanning orbits 001330–003824 were analyzed sequentially by orbit number ( $\sim 530$  images). Next, a subset of images from orbits 003825–006981 were selected on the basis of geographical location within the  $30\text{--}80^\circ$  latitude bands in order to increase the density of analyzed images in locations sparsely sampled in early orbits. A sense of image clustering is given by mean nearest-neighbor distances between images: 133 km for northern hemisphere images and 94 km for southern hemisphere images. HiRISE images are targeted to features, areas, and to regional characterization. Although image distribution is not strictly random, we feel that the combination of sequential and gap-filling images is representative of a wide variety of high-latitude surfaces.

[8] In order to distinguish thermal contraction crack polygons from nonperiglacial/permafrost features, we evaluated

**Table 1.** Summary of Morphometric and Distribution Characteristics for Small-Scale Polygons Present in the Martian Latitude-Dependent Mantle<sup>a</sup>

Morphological Group	Mean Diameter NH/SH <sup>b</sup> (m)	Identifying Characteristics	Latitude Range NH/SH <sup>b</sup> (Degrees)	Type Locality HiRISE Image NH/SH <sup>b</sup>
High-Relief	6.1/5.6	Deep and variably wide troughs around high centers	67–72°N/70–80°S	PSP_001474_2520/PSP_002928_1035
Flat-Top Small	5.2/10.6	Crisp troughs around flat, high centers	65–73°N/47–79°S	PSP_001959_2485/PSP_003998_1105
Irregular	5.6/18.3	Poorly polygonalized, throughgoing features	62–69°N/55–71°S	PSP_001959_2485/PSP_001831_1155
Subdued	16.0/16.8	Broad troughs and gently sloping high centers	45–62°N/44–71°S	PSP_002320_2360/PSP_003818_1360
Gullygons	11.0/9.3	Polygons stratigraphically linked to gullies	37–73°N/33–72°S	PSP_001357_2200/PSP_001882_1410
Peak-Top	9.1/8.9	Steeply convex up interiors, narrow troughs	41–56°N/44–55°S	PSP_001737_2250/PSP_003217_1355
Mixed Center	11.0/9.9	High, flat interiors transition to low, flat interiors	32–57°N/35–59°S	PSP_002175_2210/PSP_002560_1335

<sup>a</sup>Diameters were calculated using polygon center to center point measurements. Latitude range is the latitude span in which a given morphological class is found. Type locality indicates a HiRISE image that contains a typical example of the morphological class. A complete list of analyzed images and classifications is included in the Auxiliary Material.

<sup>b</sup>NH, northern hemisphere; SH, southern hemisphere.

all occurrences of polygonally patterned ground observed in the surveyed HiRISE images using a series of criteria which can be used to distinguish the origin of polygonal surfaces from orbital imagery. Criteria used to identify thermal contraction crack polygons on Mars are detailed in the Appendix A.

### 3. Polygon Classification and Distribution

[9] In the following subsections, we present descriptions of seven morphological varieties of small-scale (<~25 m diameter) contraction crack polygons on Mars (Table 1). The goal of this classification is to provide a nomenclature for identifying and discussing polygonally patterned ground on the basis of morphological characteristics that are readily apparent from inspection of HiRISE image data. Polygon classification is based on identifying morphological characteristics observable in full-resolution HiRISE images. Identifying characteristics include polygon diameter and topography, polygon trough size and steepness, surface texture, rock cover distribution, and interactions with adjacent or underlying landscape features. Some identifying characteristics may not be apparent in down sampled or highly compressed images.

[10] Morphological classes of polygonally patterned ground are named on the basis of surface morphological characteristics. In contrast, polygons in terrestrial permafrost environments are classified and named on the basis of subsurface structure and wedge composition, resulting in the familiar ice wedge, sand wedge, and sublimation polygon types [e.g., *Pewe*, 1959, 1963; *Berg and Black*, 1966; *Washburn*, 1973; *Marchant and Head*, 2007]. Limited access to the subsurface of Martian polygonally patterned ground necessitates a broader morphological approach that will continue to be refined by future subsurface investigations [*Smith et al.*, 2007].

[11] Polygons are common at Martian middle-high latitudes (30–80°): 276 of 413 northern hemisphere images and 207 of 410 southern hemisphere images feature at least one morphological class of polygonally patterned ground (Figure 1). It is common for more than one variety of polygonally patterned ground to be present in a single HiRISE image. Polygon diameters are reported on the basis of polygon center to center measurements, averaged across the four nearest polygon centers for each polygon measured, and then averaged across a set of >100 polygons per morphological class. Large-scale, multikilometer polygonal structures [e.g., *Hiesinger and Head*, 2000] are not considered in this study. A complete database of analyzed images,

including a list of morphological classes of polygonally patterned ground present in each image, is included in the Auxiliary Material.<sup>1</sup>

#### 3.1. High-Relief Polygons

[12] High-relief polygons (HR) have strong topographic contrasts between polygon interiors and topographically depressed, straight-sided polygon troughs (Figure 2). HR are morphologically similar to S1 terrain described by [*Mangold*, 2005], with diameters averaging 6.1 m in the northern hemisphere, and 5.6 m in the southern hemisphere. HR are commonly clustered into groups of polygons with relatively shallow and narrow troughs that are outlined by wider and deeper troughs. HR trough intersections are commonly both near orthogonal and near hexagonal. HR polygons are common at high northern latitudes (present in 21 images in the northern hemisphere with a distribution centered at 69°N) and less common in high southern polar latitudes (present in 6 images in the southern hemisphere with a distribution centered at 75°S).

#### 3.2. Flat-Top Small Polygons

[13] Flat-top small polygons (FTS) are the predominant northern hemisphere polygon class (present in 119 images) and a significant population in the southern hemisphere (present in 48 images, Figure 3). FTS polygons are all broadly similar to the S group described by *Mangold* [2005]. FTS were first described in proximity to the NASA Phoenix landing site [*Mellon et al.*, 2007; *Arvidson et al.*, 2008; *Levy et al.*, 2008b; *Mellon et al.*, 2008]. FTS (Figure 3) are straight-sided polygons (mean diameter 5.2 m in the northern hemisphere, 10.1 m in the southern hemisphere) with visible, negative trough relief. FTS trough intersections are commonly both near orthogonal and near hexagonal, outlining relatively flat-topped, high-center polygons. FTS polygon troughs form sharply defined networks of fractures (Figure 3). Frost seasonally accumulates in FTS troughs, and may be preserved into the spring season. Boulder piles are present overlying approximately 40% of northern hemisphere FTS polygons, forming “basketball terrain” light and dark patterns observed in MOC images [*Malin and Edgett*, 2001; *Mellon et al.*, 2007]. Basketball terrain caused by boulder piles is absent in southern hemisphere images analyzed in this survey. FTS distribution is centered on 68.6°N in the northern hemisphere, and on 64.0°S in the southern hemisphere.

<sup>1</sup>Auxiliary material data sets are available at <ftp://ftp.agu.org/apend/j/e/2008je003273>.

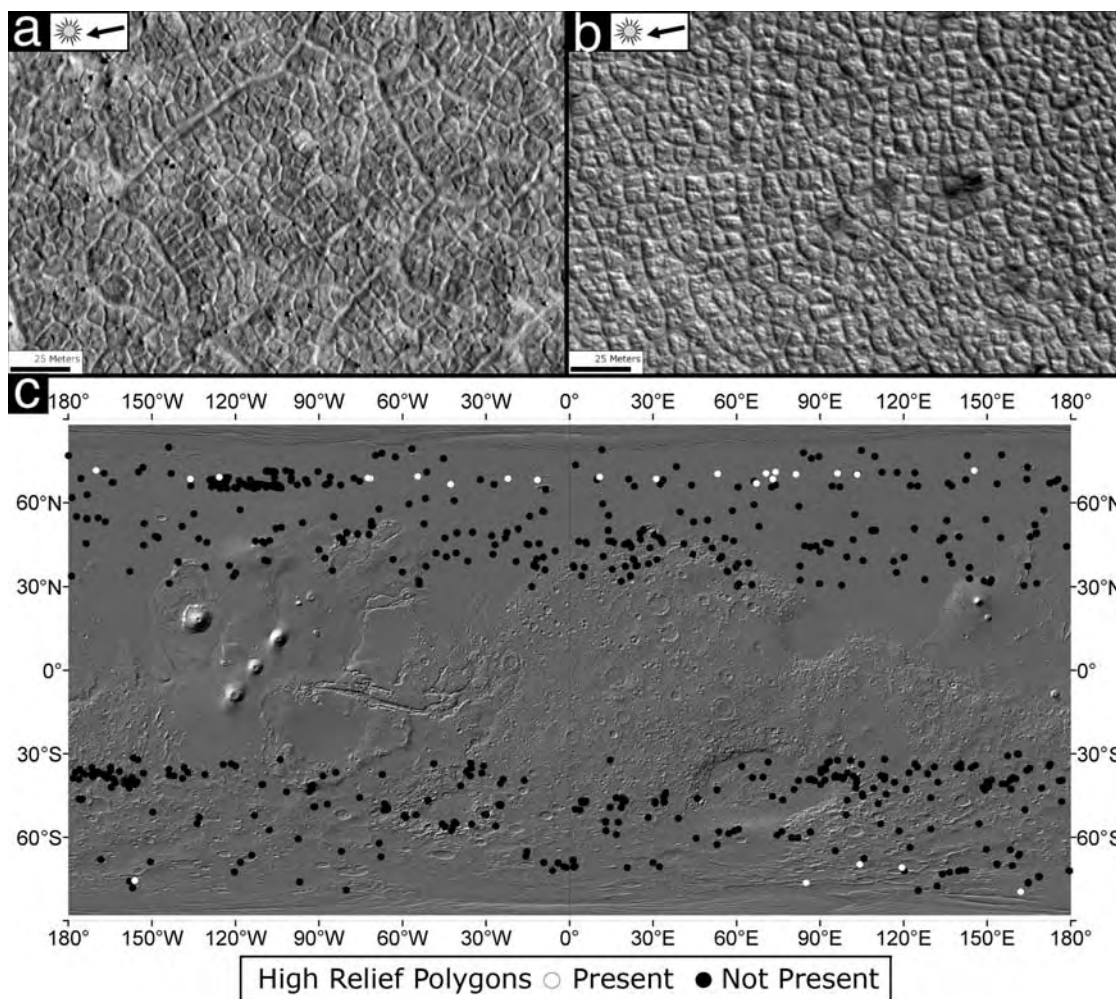


**Figure 2.** (a) An example of high-relief polygons in the northern hemisphere. Polygons are high centered with deep bounding troughs of variable width. Illumination is from the right. Portion of image PSP\_001474\_2520. (b) An example of high-relief polygons in the southern hemisphere. Illumination is from the right. Portion of HiRISE image PSP\_002928\_1035. (c) Distribution map of high-relief polygons. High-relief polygons are most prevalent at high-polar latitudes.

### 3.3. Irregular Polygons (IRR)

[14] Irregular polygons (IRR) are composed of poorly polygonalized networks of fractures, commonly consisting of long, sinuous cracks (some of which have raised shoulders) and smaller, polygon-forming fractures (Figure 4). IRR trough intersections are commonly near orthogonal. IRR have a distinctly “wormy” surface texture on account of the longer, throughgoing fractures (Figure 4). Where well-formed IRR polygons are present, they are commonly flat topped, with high centers; however, IRR polygons are most commonly outlined by incomplete fracture networks, giving them a degraded appearance (Figure 4). IRR are typical of the Phoenix landing site [Arvidson *et al.*, 2008; Mellon *et al.*, 2008; Smith, 2008]. IRR are present in 83 images in the northern hemisphere (centered on 67°N) and are present in 18 images in the southern hemisphere (centered on 65°S, Figure 4).

### 3.4. Subdued Polygons (SUB)

[15] Subdued polygons (SUB) average 16 m in diameter in the northern hemisphere and 16.8 m in diameter in the

southern hemisphere (Figure 5). SUB polygons are bounded by depressed troughs that are broader (up to 1–2 m) and less straight than those outlining FTS polygons, making them broadly similar to Mangold [2005] S3 polygons. SUB polygon troughs are commonly lighter toned than polygon interiors. Subdued polygon interiors are commonly flat, to gently convex up. SUB commonly have small, ~1-m-scale boulders accumulated in interpolygon troughs, forming networks of lineated boulders. Subdued polygon trough intersections are commonly near hexagonal. SUB polygons are present in 38 images in the northern hemisphere (distributed in a range centered on 54°N) and are present in 16 images in the southern hemisphere (distributed in a range centered on 57°S, Figure 5).

### 3.5. “Gullygons” (Gully Polygon Systems)

[16] “Gullygons” (Figures 6 and 7) are polygons that are present in gully alcoves, along gully channels, or that interact with gully fans [Levy *et al.*, 2008a, 2009b]. Gullygons are commonly flat centered with sharply defined, bounding troughs, forming polygons which average ~11 m in diameter

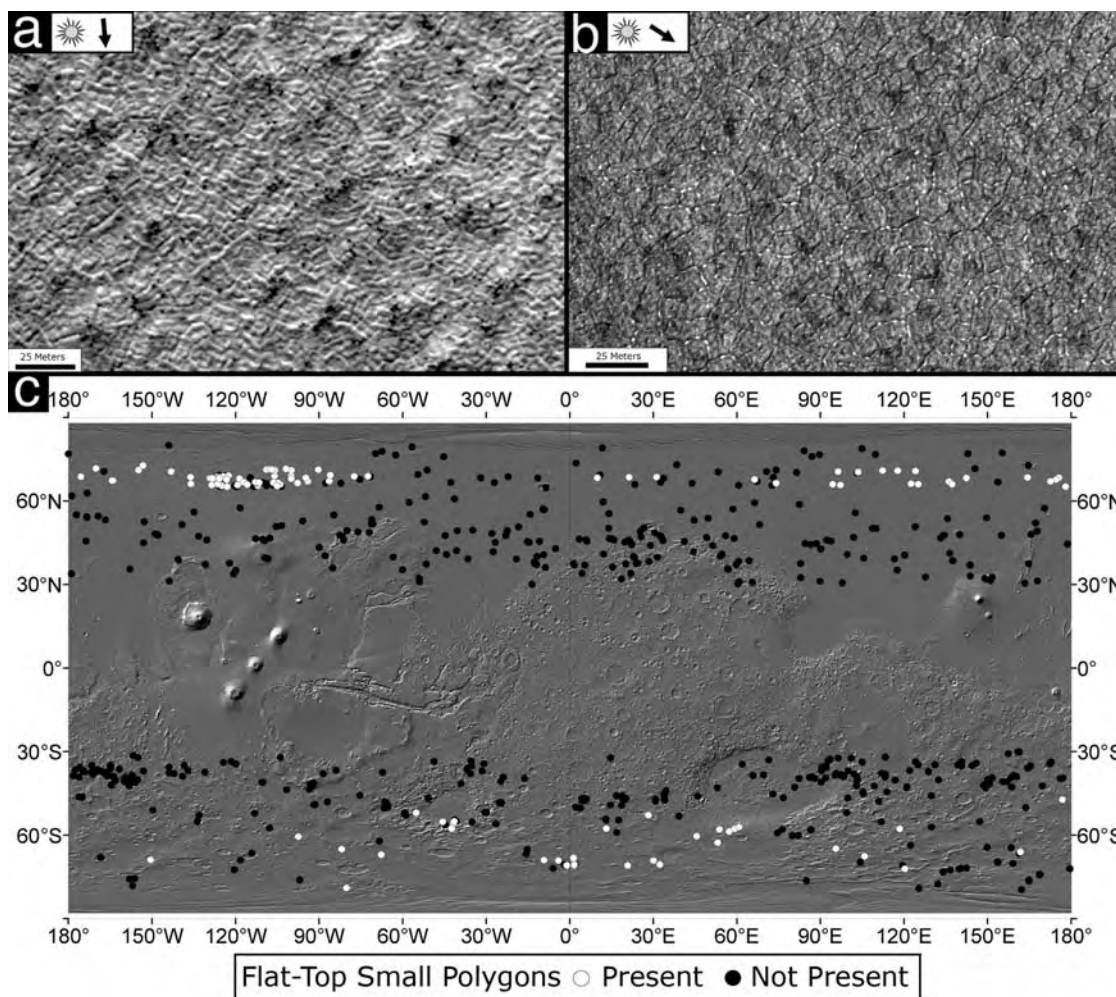


**Figure 3.** (a) Flat-top small polygons in the northern hemisphere. FTS polygons are high centered with clearly demarcated bounding troughs surrounding relatively flat-lying interiors. Illumination is from image top. Portion of image PSP\_001959\_2485. (b) Flat-top small polygons in the southern hemisphere. Illumination from upper left. Portion of image PSP\_003998\_1105. (c) Global distribution map of flat-top small polygons. FTS are clustered in the northern plains and are more broadly distributed in the southern hemisphere.

in the northern hemisphere and 9.3 m in diameter in the southern hemisphere. Gullygon trough intersections are commonly near orthogonal, particularly when gullygons are present on slopes. Stratigraphic relationships within gully polygon systems indicate that polygon development both precedes and postdates gully activity in some images containing gullygons [Levy *et al.*, 2009b] (Figure 7). Gullygons are rare in the northern hemisphere, and are present in 25 images, spanning a range centered on 51°N (Figure 6). Gullygons are common in the southern hemisphere, and are present in 91 images, spanning a range centered on 47°S (Figure 6).

### 3.6. Peak-Top Polygons

[17] Peak-top polygons (PT) are characterized by steeply peaked or pointed, convex up polygon interiors (Figure 8). Shadow measurements indicate that PT polygon interiors can be inclined up to  $\sim 30^\circ$ . PT are bounded by shallow, narrow polygon troughs. Peak-top polygons average 9.1 m in diam-

eter in the northern hemisphere and 8.9 m in the southern hemisphere. PT trough intersections are commonly near orthogonal. PT form in association with mixed center polygons (below) as well as in isolation. PT are present in 22 images in the northern hemisphere (distributed in a range centered on 49°N) and are present in 13 images in the southern hemisphere (spanning a range centered on 52°S, Figure 8).

### 3.7. Mixed Center Polygons

[18] Mixed center polygons (MX) are one of the most pervasive classes of polygons on Mars. MX polygons have two distinct forms which transition into one another over meter length scales: high center and low center. High-center MX polygons are composed of depressed surface troughs that intersect at both near-orthogonal and near-hexagonal intersections, forming polygons with topographically high interiors relative to their boundaries (Figure 9). High-center MX polygon interiors are commonly flat topped to slightly convex up. Low-center MX polygons are composed of troughs

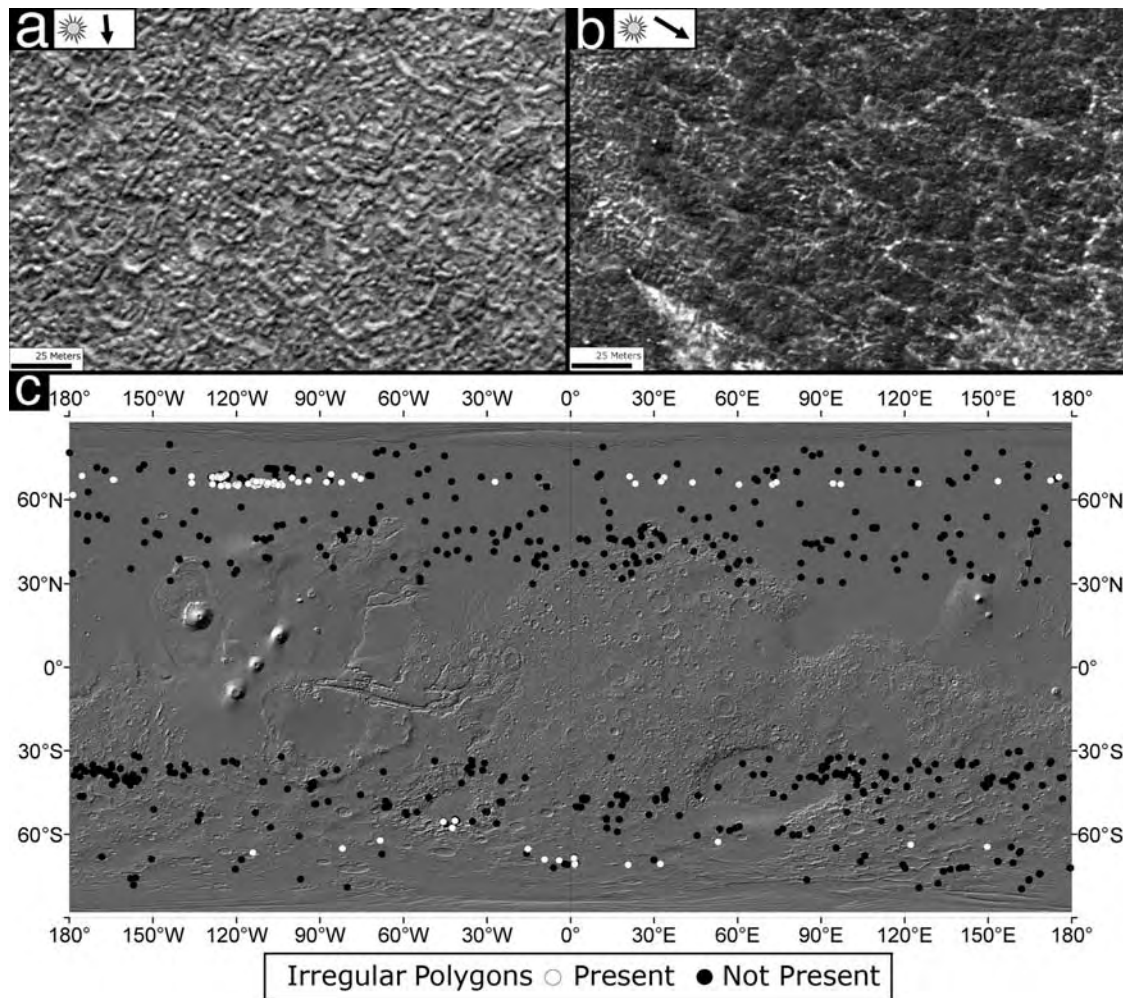


**Figure 4.** (a) Irregular polygons in the northern hemisphere. IRR are poorly polygonalized and may contain throughgoing fractures  $\sim 100$  m long, in addition to meter-scale polygons. Some large IRR fractures have slightly raised shoulders. Illumination is from image top. Portion of image PSP\_001959\_2485. (b) Irregular polygons in the southern hemisphere. Illumination is from image top. Portion of image PSP\_001831\_1155. (c) Distribution map of irregular polygons. IRR are concentrated in the equatorward portions of the northern plains and are more broadly distributed in the southern hemisphere.

with raised shoulders that intersect at near-orthogonal and near-hexagonal intersections, forming polygons with depressed centers, relative to the raised rims (Figure 9). Low-center MX polygons have smooth, flat, depressed interiors. Low-center MX polygons occur predominantly on steep-walled, scalloped depressions and on mantled slopes adjacent to “brain terrain” surfaces [Dobrea *et al.*, 2007; Levy *et al.*, 2009a]. MX polygon diameter is approximately constant between high- and low-center forms, averaging 11.3 m in the northern hemisphere and 9.9 m in the southern hemisphere. MX polygons are present in 57 northern hemisphere images (centered on 43.3°N) and in 76 images in the southern hemisphere (centered on 44.6°S, Figure 9). Polygons similar to the MX group have been identified in and around the enigmatic scallops in Utopia Planitia [e.g., Kanner *et al.*, 2004; Soare *et al.*, 2008], and in circum-Hellas and Argyre terrains [Lefort *et al.*, 2007; Morgenstern *et al.*, 2007; Costard *et al.*, 2008; Zanetti *et al.*, 2008], as well as in latitude-

dependent mantle deposits overlying lineated valley fill and concentric crater fill [Dobrea *et al.*, 2007; Levy *et al.*, 2009a].

#### 4. Polygonally Patterned Surface Age Distributions

[19] Understanding the ages of polygonally patterned surfaces on Mars is critical for assessing the duration and nature of climate conditions resulting in the emplacement of ice at high Martian latitudes, and the subsequent modification of those ice rich terrains. Estimates of the age of polygonally patterned, Martian latitude-dependent mantle surfaces range from 0.1 Ma [Kostama *et al.*, 2006] to  $\sim 1$  Ma [Mangold, 2005]; generally consistent with estimates of ages for the Martian latitude-dependent mantle spanning  $10^5$ – $10^7$  years [Milliken *et al.*, 2003].

[20] Previous age estimates are derived from crater counts using Mars Orbiter Camera images that commonly have a

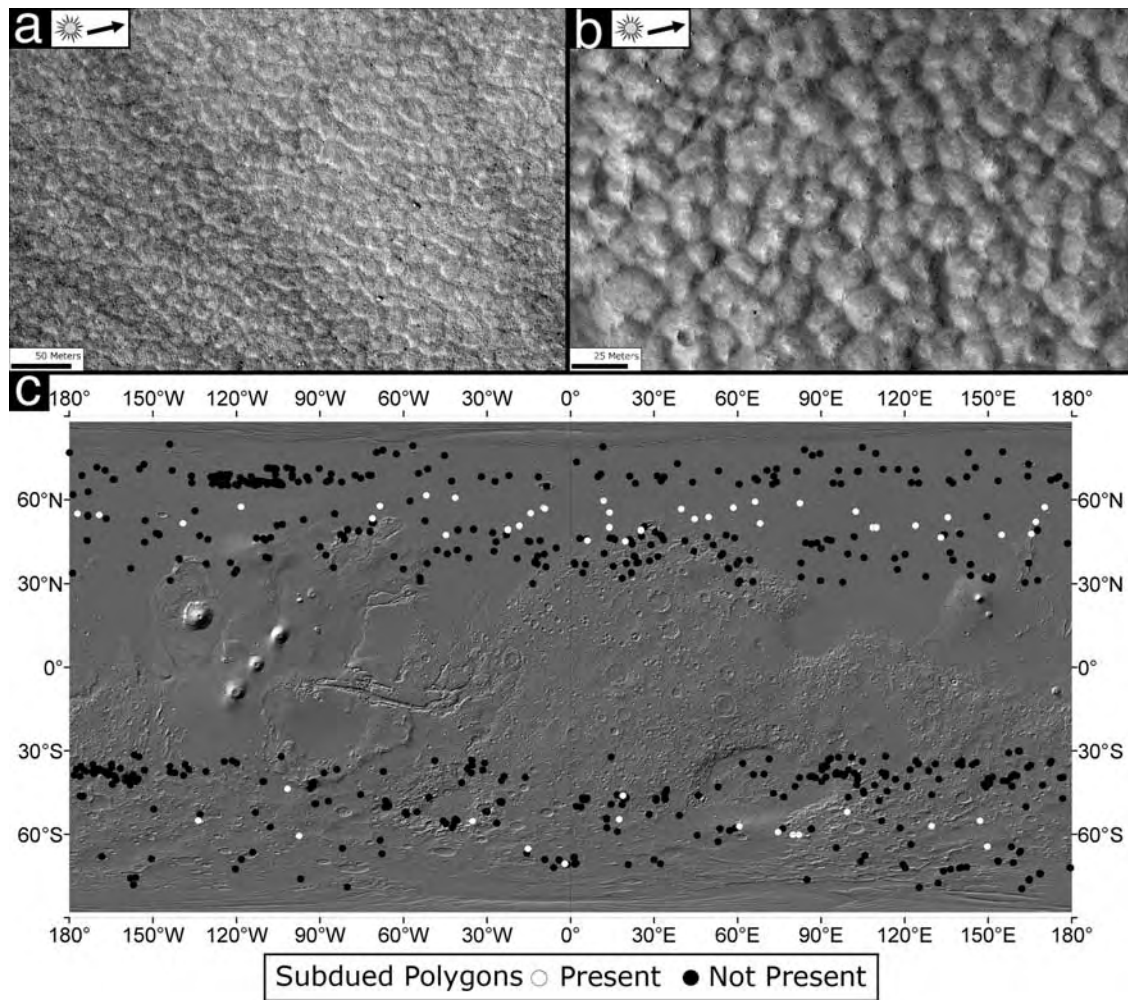


**Figure 5.** (a) Subdued polygons in the northern hemisphere. Subdued polygons are commonly bounded by broad, shallow troughs. Meter-scale boulders may be accumulated in the troughs. Illumination is from the lower left. Portion of image PSP\_001481\_2410. (b) Subdued polygons in the southern hemisphere. SUB are generally larger than HR, FTS, and IRR polygons and have broad troughs between topographically high polygon centers. Illumination is from the lower left. Portion of image PSP\_003818\_1360. (c) Distribution map of SUB polygons. Subdued polygons are typical of Martian midlatitudes.

spatial resolution of  $\sim 3\text{--}6$  m/pixel; HiRISE images of similar terrains are up to an order of magnitude higher in spatial resolution, permitting precise measurement of small craters 10–50 m in diameter [Hartmann, 2008; Hartmann *et al.*, 2008] that record the detailed age and modification history of polygonally patterned units. Recent estimates of the current flux of small, primary impactors indicate that primary production functions are well fitted by observed impacts with diameters as small as  $\sim 5$  m [e.g., Malin *et al.*, 2006; Hartmann, 2008; Kreslavsky, 2008]. Detection of a few pristine impact craters on polygonally patterned surfaces and identification of impact craters that have clearly been modified by polygon formation and eolian processing suggests that craters in the patterned substrate are formed, preserved and degraded in a mode similar to those formed in other materials on Mars. Accordingly, we have confidence in the crater retention ages for polygonally patterned deposits.

[21] Crater counts were conducted on three classes of polygons in the northern hemisphere: mixed center polygons,

subdued polygons, and flat-top small polygons. HiRISE images were resurveyed for crater counting at a scale of 1:3,000, readily permitting the identification of craters 5–10 m in diameter. Precise measurements of crater diameter were made at 1:300 scale by fitting a circle to the observed crater rim, and calculating a representative diameter. Where clusters of small impact craters occurred [Ivanov *et al.*, 2008], a correction was made for original impactor size using the technique outlined by Kreslavsky [2008].

[22] Crater counts were made on latitude-dependent mantle surfaces patterned by mixed center polygons (MX). Four HiRISE images in Utopia Planitia were analyzed, centered on a latitude of  $\sim 45^\circ\text{N}$ . Only fresh craters, showing no indication of modification by postimpact thermal contraction cracking were counted. Results indicate an age of  $\sim 1.5$  Ma (best fit ages span 1.3 to 1.7 Ma using Neukum and Ivanov's [2001] and Hartmann's [2005] production functions, respectively) for latitude-dependent mantle surfaces patterned by mixed center polygons (Figure 10). These results are consistent

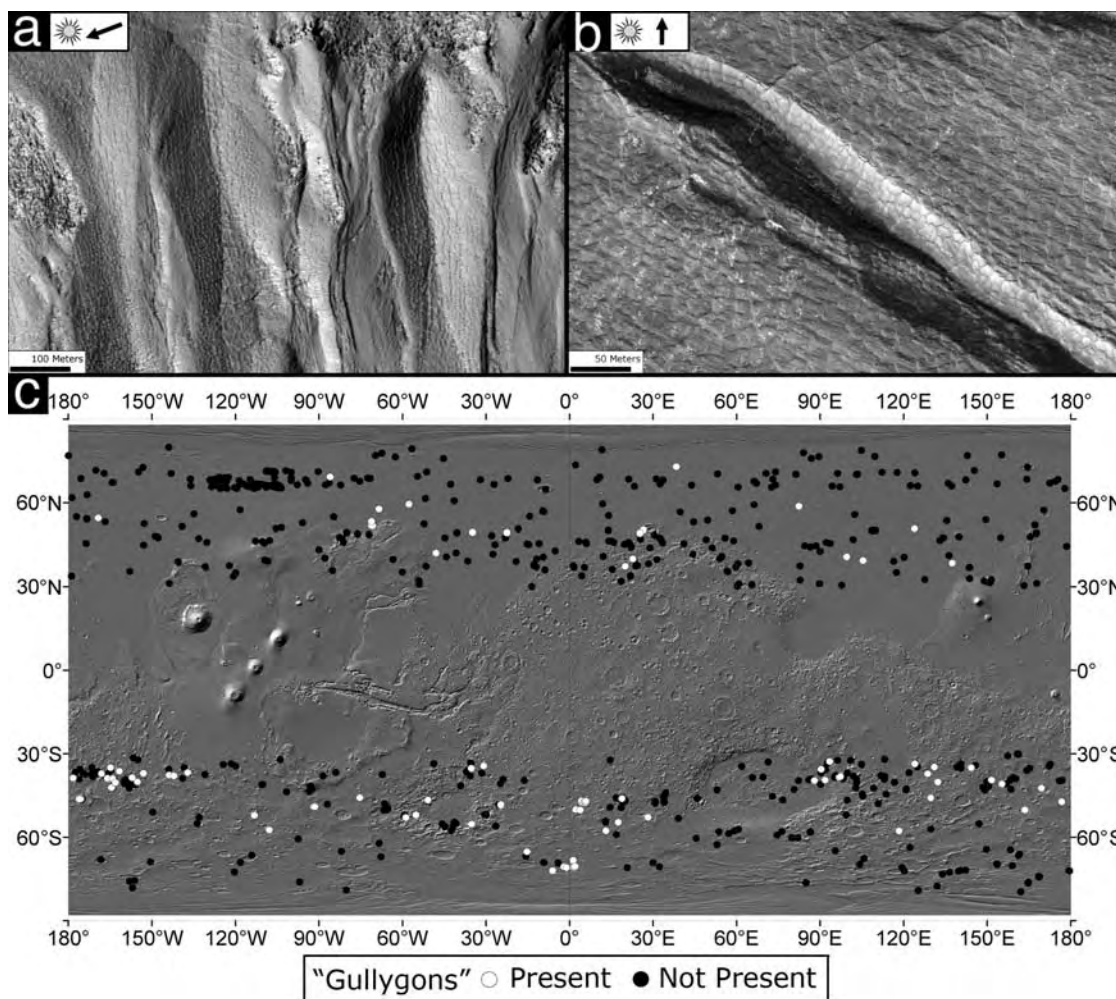


**Figure 6.** (a) Northern hemisphere gullygons or gully polygon systems. Polygons are present in alcoves of several gullies on a crater rim. Illumination is from the right. Portion of image PSP\_001357\_2200. (b) Gullygons in the southern hemisphere. Polygons entirely overprint an elongate gully alcove. Illumination is from the lower left. Portion of image PSP\_001882\_1410. (c) Distribution map of gullygons. Gully polygon systems are more common in the southern hemisphere than in the northern hemisphere.

with counts of fresh craters performed by *McBride et al.* [2005], who report young ( $\sim 1$  Ma) ages for craters that have not been modified by thermal contraction cracking (dating the most recent period of ice-rich substrate deposition). Complex ice-related stratigraphy in terrains surfaced by mixed center polygons, particularly in concentric crater fill environments in Utopia Planitia [e.g., *McBride et al.*, 2005; *Levy et al.*, 2009a] suggest glacial and polygon-forming activity of increasing ages up to  $\sim 100$  Ma.

[23] Crater counts were conducted on seven HiRISE images exhibiting subdued polygons. Images were distributed throughout a latitude band centered on  $\sim 55^\circ\text{N}$ . Only fresh craters, showing no indication of postimpact thermal contraction crack modification were included in these measurements. Results indicate an age of  $\sim 130$  ka (best fit ages span 80 to 190 ka using *Neukum and Ivanov's* [2001] and *Hartmann's* [2005] production functions, respectively) for fracturing of surfaces showing subdued polygons (Figure 10).

[24] Crater counts were made on seven HiRISE images in which flat-top small polygons are present. Images are dis-

tributed throughout a latitude band centered on  $\sim 65^\circ\text{N}$ . Previous crater counts on similar northern plains surfaces have documented craters that were interpreted to be fresh, and unmodified by thermal contraction cracking processes [*Kostama et al.*, 2006; *Mangold*, 2005]. Inspection of small ( $< 50$  m diameter) impact craters in FTS polygon units at HiRISE resolution shows that all impact craters imaged in FTS units analyzed in this survey have been modified by thermal contraction cracking after impact crater formation. Impact crater modification consists of smoothing of impact crater rims and ejecta, filling in of impact crater bowls, and formation of thermal contraction crack polygons that are continuous with the polygon network outside of the craters (Figure 11). If there are no craters which postdate the latest period of ice-rich mantle deposition and thermal contraction cracking of FTS polygon surfaces, an estimate of the age of the surface can be derived by considering that cratering is a spatially random Poisson process [*Fassett and Head*, 2008a], a null count yields a maximum expected crater density (with 90% certainty) equal to 2.306 divided by the count area

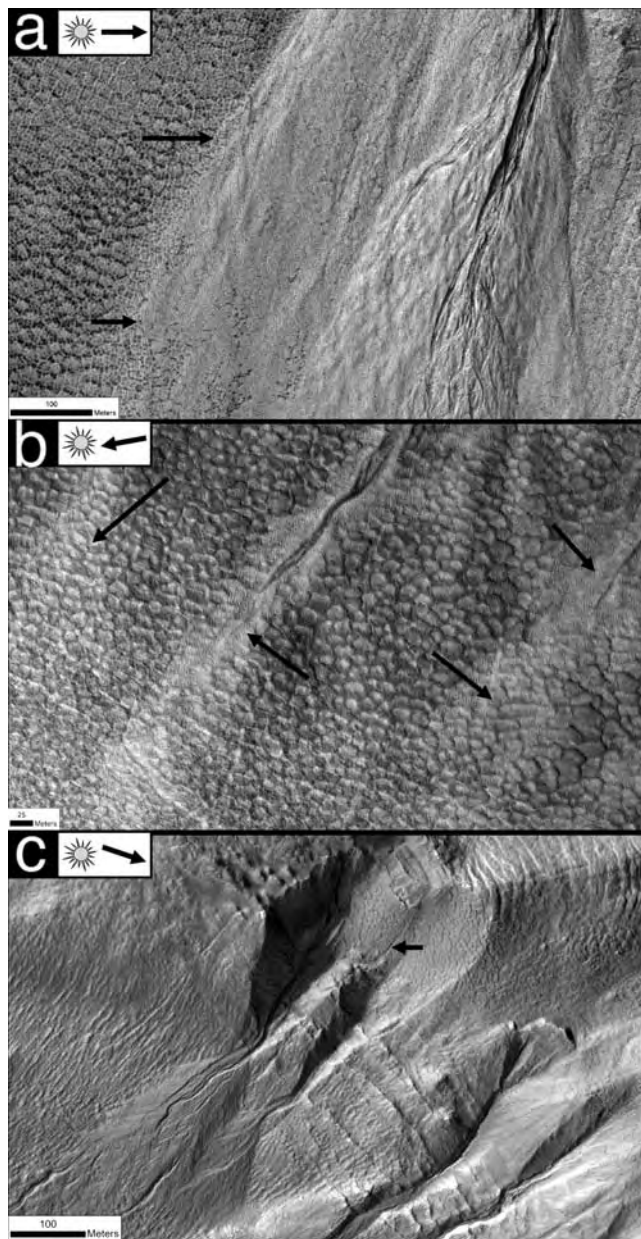


**Figure 7.** Detailed stratigraphic relationships in gully polygon systems. (a) Gully fan material overprinting polygonally patterned ground (arrows show contact). A fine network of fissures can be seen in the fan, suggesting winnowing of gully fan material by continuously expanding polygon fractures. Illumination is from the left. Portion of image PSP\_002368\_1275. (b) Small gully fans overprinting polygonally patterned ground (arrows). The presence of light-toned fan material on polygon interiors but not preferentially accumulated in polygon troughs, suggests that in this location polygon formation postdates fan deposition. Illumination is from the upper left. Portion of image PSP\_001846\_2390. (c) Polygons present in the alcove of a large gully. Arrow indicates a channel present between polygon interiors, interpreted to indicate annexation of polygon troughs by the gully channel. Illumination is from the upper left. Portion of image PSP\_001714\_1415.

( $\sim 585 \text{ km}^2$  for images containing FTS polygons) [Kreslavsky, 2008]. By determining the minimum crater diameter at which we are confident that there are zero unmodified craters in FTS polygon terrains ( $\sim 20\text{--}30 \text{ m}$ ) we arrive at a maximum age of  $\sim 50\text{--}100 \text{ ka}$  for the most recent period of far northern hemisphere ice emplacement and polygon development (Figure 10).

## 5. Discussion

### 5.1. Geographical Patterns of Polygon Distribution

[25] One of the most striking results of mapping polygon morphological class distributions over Martian middle to high latitudes is the pronounced latitudinal (zonal) partitioning of polygon classes (Figure 12). Polygon distribution is not strongly correlated with global geological units [e.g., Skinner *et al.*, 2006]; rather, polygonally patterned ground is most commonly present in a mantling unit that overlies units representing all geological epochs (Noachian through Amazonian, see Figures 9, 11, and 13). The recent formation of polygonally patterned ground (within the past  $\sim 1\text{--}2 \text{ Ma}$ ), coupled with its formation in surface units draped over previously extant topography, strongly suggests that polygonally patterned ground represents a modification of recent Amazonian Martian latitude-dependent mantle (LDM) surfaces [e.g., Mustard *et al.*, 2001; Head *et al.*, 2003; Kostama *et al.*, 2006].

[26] On the basis of geographical distribution, small Martian polygons can be classified into two major groups: high- and low-latitude suites. High-latitude polygon classes include high-relief, flat-top small, and irregular polygons. Low-latitude polygons include peak-top and mixed center polygons. In both hemispheres, subdued and gullygon polygons bridge the latitude bands between high- and low-latitude groups. The causes of, and relationships between changes in polygon morphology across the Martian surface are discussed in subsequent sections.

[27] What are the possible causes of the strong zonal clustering of polygon morphology [e.g., Marchant and Head, 2007]? Broadly, the distribution of small Martian polygons is consistent with the extent of the Martian latitude-dependent mantle: a unit interpreted to originate from the deposition and modification of tens of meters of atmospherically emplaced ice and sediments [Mustard *et al.*, 2001; Kreslavsky and Head, 2002; Head *et al.*, 2003; Milliken *et al.*, 2003]. In particular, high-latitude polygon groups are found at latitudes broadly characterized as “intact mantle” ( $>60^\circ$  latitude), and low-latitude polygons are found within “dissected mantle” terrains ( $\sim 30\text{--}60^\circ$  latitude) [Milliken *et al.*, 2003]. Gullygons, and to a lesser extent, subdued polygons, straddle this boundary [Levy *et al.*, 2009b]. Whether intact, or dissected, the Martian LDM is the primary substrate in which small-scale thermal contraction crack polygons form on Mars, owing to the combination of near-surface ice that responds to seasonal thermal contraction [Mellon and Jakosky, 1995; Mellon, 1997] with fine-grained sediment: optimum conditions for thermal contraction crack polygon formation and development [Washburn, 1973; French, 1976; Yershov, 1998].

### 5.2. Polygon Generation Processes and Conditions

[28] In terrestrial thermal contraction crack polygons, morphological development is largely dependent on subsurface rheological properties (including ice content), and surface

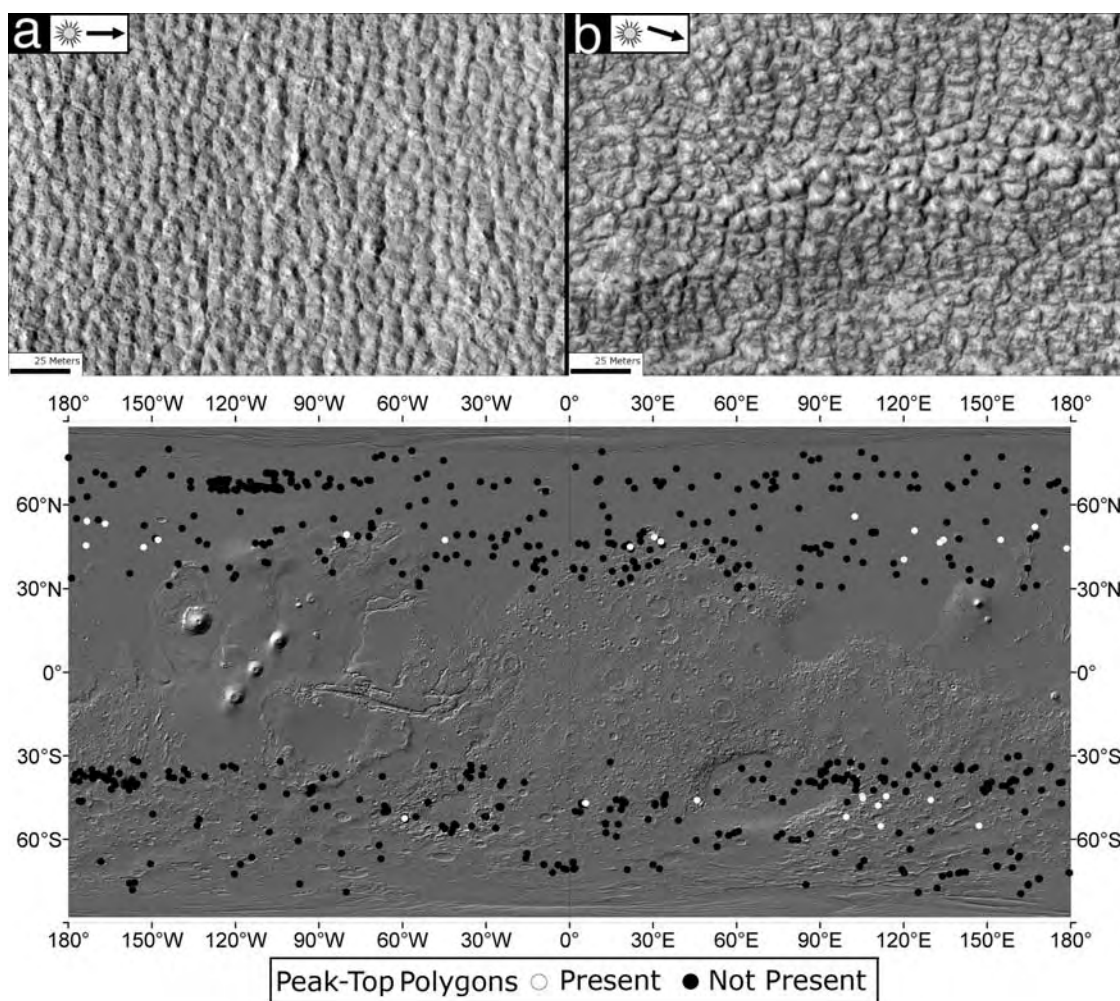


**Figure 8.** (a) Peak-top polygons in the northern hemisphere. PT are characterized by steeply sloped, convex up polygon interiors. Illumination is from the left. Portion of image PSP\_01737\_2250. (b) PT polygons in the southern hemisphere. Illumination is from the left. Portion of image PSP\_003217\_1355. (c) Distribution map of PT polygons. PT are typical of Martian middle-low latitudes and may form in association with mixed center polygons.

environmental factors, including the presence or absence of saturated active layers [Pewe, 1959; Lachenbruch, 1961; Maloof et al., 2002; Marchant and Head, 2007]. In wet climates, in which a typical active layer is present, ice wedge polygons commonly develop [Berg and Black, 1966; Washburn, 1973]; in cold and dry climates, in which soil conditions are too dry to develop traditional wet active layers, sand wedge polygons may form [Pewe, 1959; Berg and Black, 1966]. Sublimation polygons are a special type of sand wedge polygon that form where excess ice (ice exceeding available pore space) occurs in the shallow subsurface [Marchant et al., 2002; Levy et al., 2006; Marchant and Head, 2007]. The strong dependence of polygon type on climate and subsurface ice conditions means that polygon types can be used as an equilibrium landform to chart spatial and temporal variation in local environmental conditions [Black, 1952; Marchant and Head, 2007].

[29] Given that access to the subsurface of Martian thermal contraction crack polygons is only accessible at select lander sites [Mutch et al., 1977; Smith, 2008], we investigate the

possibility that surface morphology can be used as an indicator of subsurface processes related to polygon development. The morphology of terrestrial thermal contraction crack polygons provides a baseline for comparison [Sletten et al., 2003; Marchant and Head, 2007]. Active ice wedge polygons are commonly outlined by troughs flanked by raised rims resulting from the displacement of soil or sediment by the growing ice wedge [Berg and Black, 1966; Black, 1982; Yershov, 1998]. Likewise, active sand wedge polygons are commonly characterized by the presence of raised shoulders flanking polygon troughs [Pewe, 1959; Murton et al., 2000]. Composite wedge polygons result from a combination of sand and ice wedge growth, generating alternating wedge lenses of ice and sand, forming polygons with both raised, and nonraised shoulders [Berg and Black, 1966; Ghysels and Heyse, 2006; Levy et al., 2008a]. Active sublimation polygon surface morphology consists of convex up, to conical, mounds of sediment-covered ice bounded by deep, nonraised rim troughs [Marchant et al., 2002; Marchant and Head, 2007].

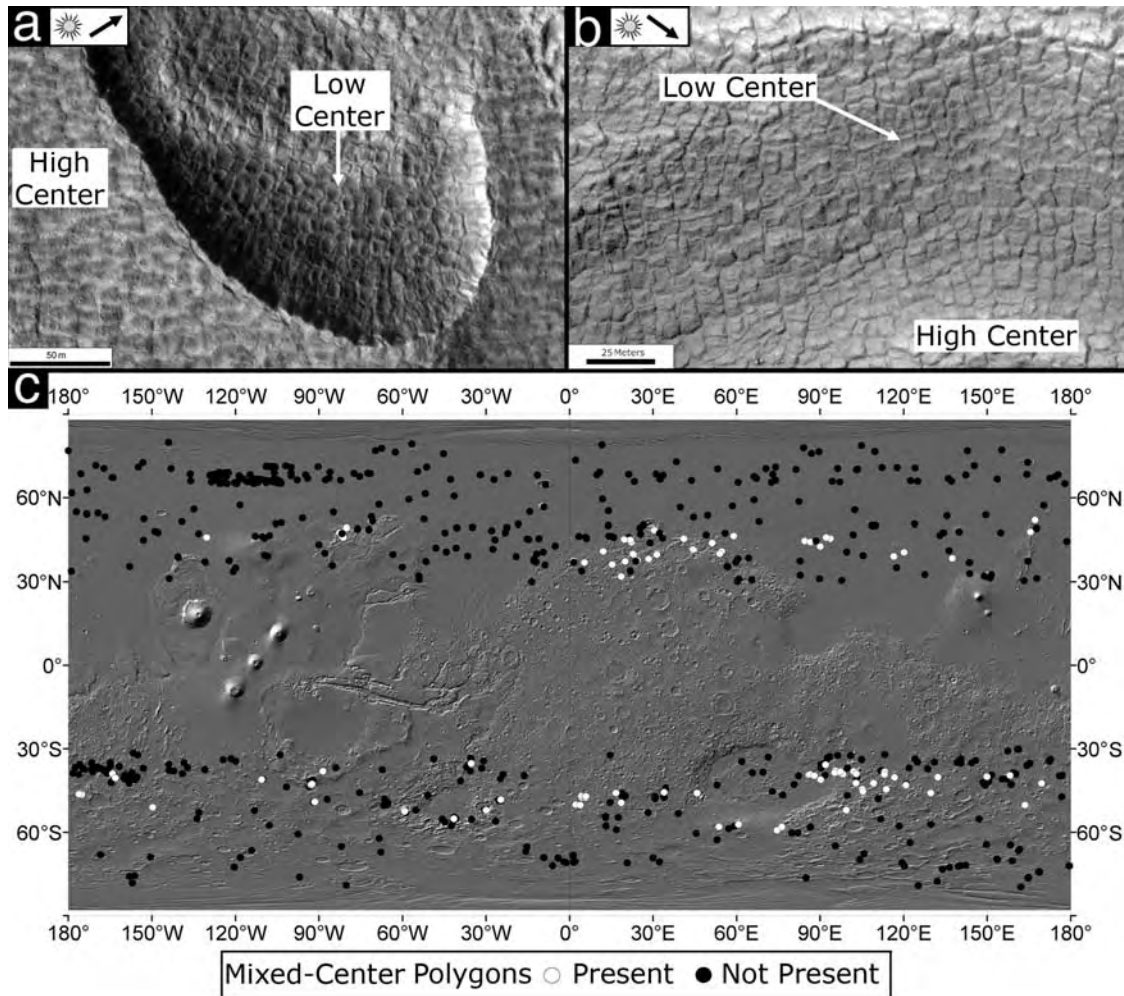


**Figure 9.** (a) Mixed center polygons in the northern hemisphere. MX are most commonly high centered with depressed bounding troughs. However, low-centered MX polygons with raised shoulders occur in scalloped depressions or on slopes in MX-patterned terrain. Illumination is from the lower right. Portion of image PSP\_002175\_2210. (b) Mixed center polygons in the southern hemisphere. Illumination is from upper left. Portion of image PSP\_002560\_1335. (c) Distribution map of MX polygons.

[30] The most striking morphological characteristic of Martian polygonally patterned ground at HiRISE resolution is the abundance of high-centered polygons that lack raised shoulders marginal to polygon troughs. Noting the predominance of high-center polygons, in addition to asymmetries in surface topography consistent with orientation-dependent differential sublimation, *Levy et al.* [2008b] interpreted polygons in the flat-top small group near to the NASA Phoenix lander site to be genetically analogous to terrestrial sublimation polygons; proximal irregular polygons were interpreted to be transitional structures between sublimation and sand wedge polygons, with the presence of occasional raised rim features in irregular polygons indicative of locally reduced ice content relative to sediment content in the cracking substrate. High-relief polygons, and southern hemisphere FTS polygons were not directly considered by *Levy et al.* [2008b], however, the high-center morphology of high-relief and southern hemisphere FTS polygons, coupled with depressed bounding troughs, also suggests loss of excess ice at polygon troughs by preferential sublimation [*Marchant*

*et al.*, 2002; *Kowalewski et al.*, 2006]. Polygon morphological classes distributed at lower latitudes also display a convex up morphology, including subdued polygons, many gullygons, peak-top polygons, and some mixed center polygons. Martian thermal contraction crack polygons are expected to be currently active, undergoing seasonal thermal contraction and fracture opening in equilibrium with present Martian conditions [*Mellon*, 1997].

[31] Taken together, these lines of evidence strongly suggest that the ice-rich substrate in which high-center polygons form (the Martian latitude-dependent mantle) is not merely ice rich, but in many places contains ice exceeding available pore space, resulting in sublimation polygon-like morphology and microtopography (high center). Further, the lack of raised rims on these polygon morphological classes strongly suggests that most were emplaced under surface temperature conditions that did not permit the formation of a seasonal, saturated active layer. Observations from this survey predict sublimation style and traditional sand wedges to be overwhelmingly more common in the subsurface of Martian

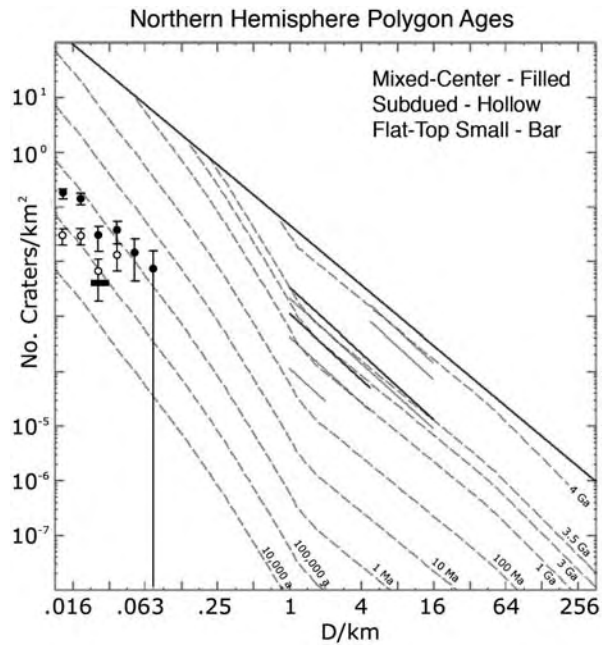


**Figure 10.** Crater retention ages of mixed center polygons, subdued polygons, and flat-top small polygons on Hartmann isochrons. MX polygons have a best-fit age of  $\sim 1.5$  Ma; SUB have a best-fit age of  $\sim 130$  ka; and the lack of nonpolygonalized craters in FTS terrains suggests that FTS surfaces may be no older than  $\sim 50$ – $100$  ka.

polygonally patterned terrains than ice wedges or ice wedge pseudomorphs. Detailed observations of polygon morphology, coupled with surface dating of northern hemisphere polygonally patterned surfaces, suggests that cold, dry conditions have persisted for at least the past  $\sim 1$ – $2$  Ma on Mars. These interpretations are consistent with observations made by the Phoenix lander [Smith, 2008] of ice-cemented soil featuring thermal contraction crack polygons and of geochemical profiles suggesting the preservation of soluble chemical species by hyperarid, cold polar conditions.

### 5.3. Polygon Morphology and Liquid Water Activity

[32] The occurrence of gully polygon systems on Mars [Head *et al.*, 2008; Levy *et al.*, 2008a, 2009b], coupled with the presence of low-center members of the mixed center polygon morphological class, raises the possibility of some role for liquid water and/or freeze-thaw processing in the formation of Martian thermal contraction crack polygons. Which observed polygon morphologies require the presence of liquid water during polygon development, and which can be accounted for by solid-vapor phase transitions?

[33] In gully polygon systems, channel-like features that are (1) continuous and sublinear; (2) present in widened, curved, and downslope-oriented gullygon troughs; and (3) present in proximity to larger, traditional gully channels, are interpreted to be remnants of polygon troughs through which liquid water flowed and deposited sediments [Head *et al.*, 2008; Levy *et al.*, 2009b] (Figure 7). Further, the propagation of some gullygon fractures upward through younger fan deposits emplaced on top of these polygons [Levy *et al.*, 2009b] suggests that some gullygons may have actively undergone seasonal thermal contraction and wedge

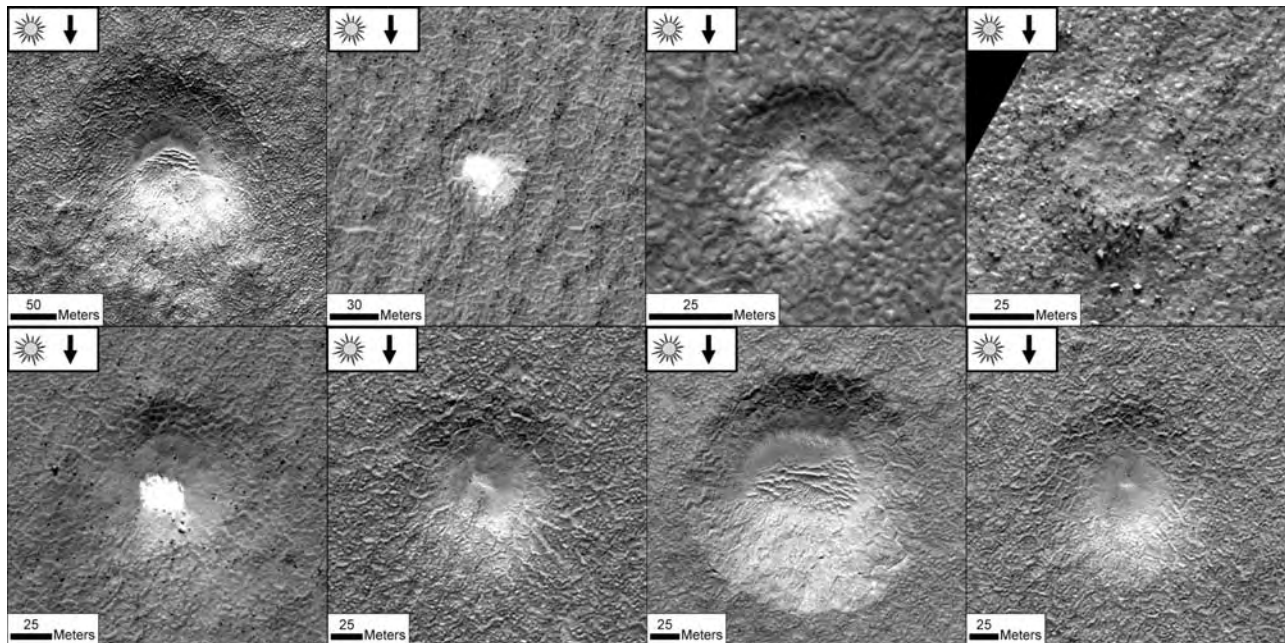


**Figure 11.** Examples of impact craters in terrains surfaced by FTS polygons. All craters have been mantled by a material that has undergone thermal contraction cracking and polygon development subsequent to crater formation. In all images illumination is from the top. Craters are selected from HiRISE images PSP\_001404\_2490, PSP\_001497\_2480, PSP\_001959\_2485, and PSP\_002170\_2485. All analyzed craters  $>25$  m in diameter have been modified by polygon-forming processes and cannot be considered “fresh.”

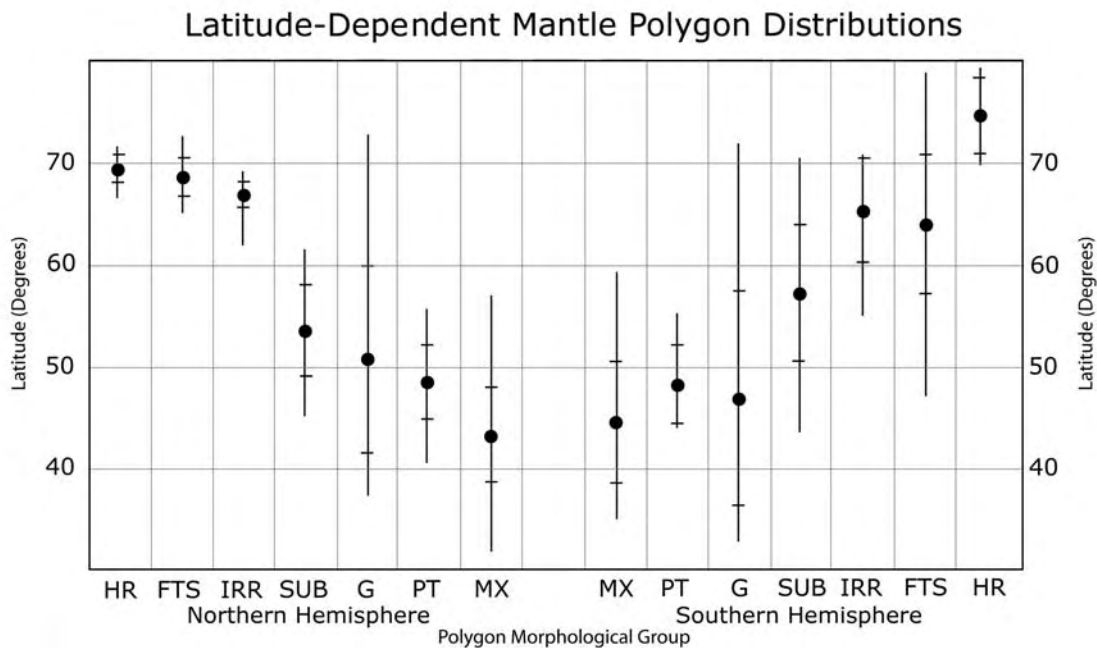


**Figure 12.** Global distribution of small Martian thermal contraction crack polygon morphological groups plotted by latitude and group. For each class we plot mean latitude of occurrence (bold circle), the range of occurrence (vertical bars), and the latitudes which bracket one standard deviation of the range of occurrence (horizontal cross bars). Polygon morphological group is a strong function of latitude and is largely symmetrical across northern and southern hemispheres, suggesting global-scale climate controls on polygon morphology.

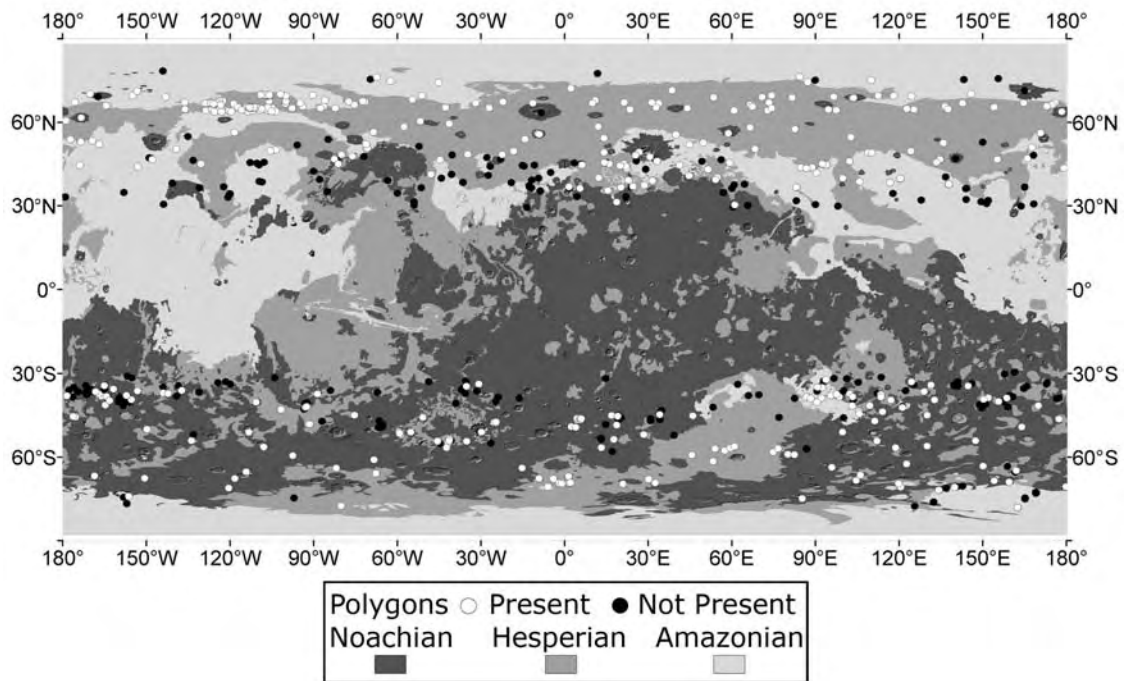


**Figure 13.** Simplified geological map showing polygon distribution over Noachian, Hesperian, and Amazonian-aged surface units, after *Skinner et al.* [2006]. Polygons are present in a geologically young mantling unit overlying surfaces of all ages. Map areas showing underlying Mars Orbiter Laser Altimeter shaded relief are not stratigraphically classified.

growth during periods of active gully flow [Levy *et al.*, 2009b] (Figure 7). The preservation of gullygons beneath some gully fans suggests that periods of gully activity were climatically warm enough to permit localized water ice melting and surface flow, but not so warm as to produce widespread active layer activity [Kreslavsky *et al.*, 2008], or complete destruction of previously emplaced polygons [Head *et al.*, 2008; Levy *et al.*, 2009b]. On the basis of these observations, we interpret gullygons to be analogous to composite wedge polygons present in the inland mixed zone of the Antarctic Dry Valleys [Marchant and Head, 2007; Levy *et al.*, 2008a], characterized by small, seasonal additions of liquid water to polygon wedges, that result in limited raised shoulder development along polygon troughs. On the basis of recent crater counts on gullied and polygonally patterned surfaces on Mars, this period of limited liquid water activity may have occurred in appropriate microclimates as recently as the past  $\sim 1.25$  Ma [Reiss *et al.*, 2004; Schon *et al.*, 2008b].

[34] To what extent are raised rims/lowered centers in some mixed center polygons indicative of the presence of liquid water or freeze-thaw cycling? Recent analyses centered in Utopia Planitia [Soare *et al.*, 2008] have concluded that terracing in scalloped depressions, coupled with the presence of polygonally patterned ground and features interpreted to be pingo scars, are indicative of late Amazonian climate conditions sufficient to produce a widespread active layer and wet thermokarst features. Alternatively, analysis of scalloped depressions in comparable surface units in Malea Planum, near the Hellas Basin [Zanetti *et al.*, 2008], have identified sublimation of buried excess ice enhanced by local wind conditions as the driving control on scalloped terrain development.

[35] Given this context, understanding how the morphological characteristics of mixed center polygons are diagnostic of geomorphic processes operating in cold and dry climates in which sublimation dominates, or in cold and wet climates, in which melting and freezing dominate, is critical to evaluating localized climate conditions at Martian midlatitudes during the late Amazonian. Levy *et al.* [2009a] have interpreted surfaces in Utopia Planitia with mixed center polygons overlying concentric crater fill deposits to be local occurrences of the Martian latitude-dependent mantle [Head *et al.*, 2003]. A similar classification of surfaces containing mixed center polygons in Melea Planum has been made by Zanetti *et al.* [2008]. The relatively high rims of some mixed center polygons (Figure 9) could be interpreted as features analogous to raised rims in active terrestrial ice wedge polygons that form either in response to displacement of soil by traditional ice wedge formation associated with the seasonal ponding and freezing of meltwater, or when ice wedge polygons are suddenly exposed to a drop in active layer water table base level: so-called, “fortress polygons” [Root, 1975]. Both of these processes require ponding of abundant meltwater, which is difficult to reconcile with the occurrence of low-center MX polygons high on the steep slopes of cusate, scalloped depressions and on mantled slopes above brain terrain that lacks evidence of modification by liquid water [Dobrea *et al.*, 2007; Levy *et al.*, 2009a].

[36] Levy *et al.* [2009a] present an alternative mechanism for the elevation of mixed center polygon shoulders that is more similar to the formation of classic sublimation polygons [Marchant *et al.*, 2002]. This model suggests that the accu-

mulation of dry wedge material in initially depressed polygon troughs eventually thickens sufficiently to insulate polygon troughs from further ice removal. Continuing sublimation is focused at less deeply insulated polygon interiors, resulting in an inversion of polygon morphology from high-center polygons to low-center polygons. Such a dry mechanism can occur effectively on equator-facing slopes which are preferentially susceptible to sublimation [Hecht, 2002], and is consistent with the preservation of proximal surfaces (e.g., brain terrain), which are  $\sim 100$  Ma old, but which do not appear to have been degraded by widespread melting and thermokarst modification [Levy *et al.*, 2009a].

[37] Is liquid water involved in any process associated with the formation of mixed center polygons? In some HiRISE images (5 images in the northern hemisphere, 24 images in the southern hemisphere) gullygons are present in images, which also have occurrences of mixed center polygons. At these sites, mixed center polygons may be modified by the ephemeral presence of gully related liquid water, forming subsurface structures analogous to terrestrial composite wedge polygons. Crater dating of these surfaces indicates that mixed center polygon formation may be contemporaneous with gully activity in certain microclimates [Levy *et al.*, 2009a; Schon *et al.*, 2008b]; however, the majority of mixed center polygons appear to have formed in isolation from conditions permitting surface flow of liquid water, and may be consistently explained by solid-vapor, cold-dry processes. In this instance, globally distributed polygonally patterned ground morphology reflects zonally averaged, cold and dry climate conditions within the past 1–2 Ma, while gully polygon interactions may reflect surface and atmospheric conditions occurring within short-lived, localized microclimate systems.

#### 5.4. Polygon Maturity and Development

[38] Do different morphological classes of Martian thermal contraction crack polygons represent (1) a continuum of development under a gradient of substrate and climate conditions, (2) unique structures and developmental histories particular to a given time or microclimate, or (3) a series of “snapshots” of a single developmental process? Answering this question is critical for evaluating the climate significance of Martian polygonally patterned ground.

#### 5.5. A Polygon Morphological Continuum

[39] The development of terrestrial thermal contraction crack polygon morphology has been studied intensely in the Antarctic Dry Valleys, both by polygon type under specified microclimate conditions over time [Marchant and Denton, 1996; Marchant *et al.*, 2002; Marchant and Head, 2007; Levy *et al.*, 2008a], as well as across polygon types and microclimate conditions [Sletten *et al.*, 2003]. These studies have shown that polygon surface appearance is strongly affected by substrate composition, climate processes particular to the microclimate in which the polygons develop, and age. We attempt to invert this analytical approach, inferring substrate properties and climate history from observed variations in the morphology of Martian polygon classes.

[40] First, we consider high-latitude polygons, particularly flat-top small and irregular (IRR) polygons (Figures 3–4): polygons typical of the Phoenix landing site and vicinity. The

morphological properties of northern hemisphere FTS and irregular polygons were used by [Levy *et al.*, 2008b] to infer that these polygons both formed by thermal contraction cracking and differential sublimation of icy substrate materials. In particular, localized differences in subsurface ice content were invoked to account for morphological differences between well-formed, FTS polygons (where ice content is greater than regolith pore space) and poorly polygonalized, occasionally raised rim irregular polygons (ice content  $\approx$  regolith pore space). FTS and irregular polygons are unique in that their narrow latitude distribution in the northern hemisphere (e.g.,  $62^{\circ}\text{N}$ – $73^{\circ}\text{N}$ ) provides a limited gradient over which zonal climate differences could affect polygon morphology. The distribution of FTS and irregular polygons is strongly affected by latitude, with FTS generally occurring more poleward than irregular polygons. This distribution is broadly consistent with decreasing water equivalent hydrogen (WEH) in the upper meter of the surface from  $\sim 25\%$  at  $70^{\circ}\text{N}$  to  $<13\%$  by  $60^{\circ}\text{N}$  [Feldman *et al.*, 2002]. This suggests that FTS and irregular polygons in the northern hemisphere may represent a continuum in polygon morphology, driven primarily by changes in substrate ice content, and secondarily by fine-scale changes in zonal climate.

[41] In contrast to those in the northern hemisphere, FTS and irregular polygons in the southern hemisphere present a more complex pattern of morphological variability. The geographical distribution of southern hemisphere FTS and irregular polygons is less tightly clustered (Figures 3–4). Southern hemisphere FTS and irregular polygon morphology and distribution may be affected by nonzonal processes, such as heterogeneous surface roughness in the southern hemisphere [Kreslavsky and Head, 2002], and variably high WEH in southern hemisphere midlatitudes [Feldman *et al.*, 2002, 2008]. Thus, southern hemisphere FTS and irregular polygons may represent a continuum of polygon morphology resulting from localized differences in substrate ice content and surface temperature differences, however, linking changes in polygon surface expression to hemisphere-scale gradients in climate or substrate properties is not possible at the present time.

### 5.6. Polygon Morphology Suggesting Unique Conditions

[42] Gullygons may represent a class of small Martian polygons that developed under unique microclimate conditions. As discussed above, the annexation of polygon troughs by gully channels, and the stratigraphic bracketing of gully fans by thermal contraction crack polygons [Levy *et al.*, 2009b] strongly suggest that liquid water was locally present during some period of gullygon development [Head *et al.*, 2008]. The absence of pronounced raised shoulders along gullygon troughs suggests that ice wedge formation was limited or did not occur in the examined gully polygon systems. The primary changes to polygon morphology resulting from interactions between polygons and gullies is the rounding of polygon trough intersections in annexed channels, and a muting of polygon trough relief where gully fans overprint and are dissected by underlying polygons. These lines of evidence suggest that milder climate conditions resulting in the formation of gully polygon systems were not warm enough to generate a widespread, deeply saturated active layer [Kreslavsky *et al.*, 2008], but were sufficient to introduce small volumes

of liquid water into polygon troughs and gully channels, analogous to the situation forming some terrestrial composite wedge polygons [Levy *et al.*, 2008a]. Water introduced into developing composite wedges is thought to be derived from the melting of atmospherically emplaced ice (either as frost or precipitated particulate ice) under peak insolation conditions [Hecht, 2002; Morgan *et al.*, 2007; Head *et al.*, 2008; Levy *et al.*, 2008a, 2009b]. In summary, even the most “extreme” warm and moist microclimate conditions which have been documented for active gully polygon systems within the past  $\sim 1$ – $2$  Ma do not result in significant changes to polygon morphology when compared to features interpreted to have formed from solid-vapor transitions, suggesting that liquid water was ephemeral, and geographically localized [e.g., Head *et al.*, 2008].

### 5.7. Polygon Morphology Suggesting Ongoing Modification

[43] Last, are there small polygons on the surface of Mars that detail steps in the developmental history of polygon morphological classes? As discussed above, transitions between high-center and low-center mixed center polygons are thought to indicate preferential removal of ice from polygon interiors following mature sediment wedge development [Levy *et al.*, 2009a]. In this manner, snapshots of polygon development are recorded in mixed center polygon morphology, with more typical, high-center examples of the polygons documenting initial stages of polygon development, and low-center examples of the polygons documenting advanced stages that highlight the effect of localized sublimation of near-surface ice at polygon centers.

[44] In summary, the characteristics of Martian polygons suggest that, like terrestrial thermal contraction crack polygons, local climate and substrate conditions have an effect on polygon expression. Higher-latitude polygons generally are more reflective of planet-scale zonal climate and buried ice gradients, while lower-latitude polygons reflect transitional morphologies, and differing stages of development. This difference suggests that latitude-dependent mantle material in which polygons form has been more recently deposited or refreshed at high latitudes, and in sheltered, southern hemisphere midlatitude locations, than at lower latitudes, consistent with crater counts of patterned terrains. Differences in polygon surface expression can assist in understanding how recently ice-rich mantling units have been deposited across a variety of Martian latitudes and microclimate zones.

## 6. Conclusions

[45] On the basis of analysis of HiRISE image data, small-scale ( $< \sim 25$  m diameter) polygonally patterned ground between latitudes  $30$ – $80^{\circ}$  on Mars has been classified into seven groups on the basis of morphological characteristics. The groups are broadly zonal, and are distributed approximately symmetrically in both the northern and southern hemispheres. Polygons are present primarily in surface units which mantle underlying topography (e.g., the Martian latitude-dependent mantle). Polygonally patterned ground on Mars is found to be primarily a mantle modification phenomenon. All observed polygon classes, with the exception of gullygons, can be interpreted to result from geomorphic processes that do not require the presence of liquid water.

Polygonally patterned units in the northern hemisphere are found to follow a strong correlation between latitude and age. Equatorward polygonally patterned units, such as mixed center polygons are the oldest ( $\sim 1.5$  Ma), followed by intermediate polygonally patterned units (e.g., subdued polygons, at  $\sim 130$  ka). Finally, high latitude northern plains polygons (e.g., FTS) are found to be the youngest ( $\sim 50$ – $100$  ka). Differences in polygon surface expression can be used as an aid in understanding how recently ice-rich mantling units have been deposited across a variety of Martian latitudes and microclimate zones—a critical step in assessing the changing habitability of Martian permafrost environments. These observations provide a global context for understanding emerging results from the Phoenix lander—particularly regarding the distribution and geological history of ice within Martian permafrost.

## Appendix A

### A1. Criteria Used to Evaluate the Thermal Contraction Crack Origin of Small-Scale Polygons on Mars

[46] Networks of fractures which intersect to form polygonal areas bounded by depressed, linear furrows, troughs, or fractures are common on Mars (Figure A1). Fractures may arise from several processes hypothesized to be active on Mars, including (1) thermal contraction of ice/ice-cemented sediments [Lachenbruch, 1962; Lucchitta, 1981; Mellon, 1997; Seibert and Kargel, 2001; Mangold, 2005; Levy et al., 2008b]; (2) thermal contraction of lava/magma [Mutch et al., 1977; Milazzo et al., 2008]; (3) desiccation (of salts, clays, or muds) [Neal et al., 1968; Seibert and Kargel, 2001; Grotzinger et al., 2006; Osterloo et al., 2008]; (4) tectonic fracture or bedrock jointing [Hiesinger and Head, 2000]; or (5) drape folding and volumetric compaction [Buczowski and Cooke, 2004]. The nature of polygonal surface features can be evaluated by application of the following morphological criteria.

#### A1.1. Network Morphology

[47] Thermal contraction cracking of permafrost, as well as (possibly) the desiccation of salts on Mars, produce episodic fracture expansion and network development, resulting in populations of proximal polygons with variable trough depths (caused by differential winnowing and ice removal) and polygon sizes (caused by variable intensity of thermal contraction and the distribution of exploitable defects) [Plug and Werner, 2001]. In contrast, desiccation of saturated sediments and cooling of surface lavas are monotonic processes, that produce a single fracture network which rarely expands or develops over time (although erosion will modify the network).

#### A1.2. Polygon Microtopography

[48] Polygons with elevated centers/sloping margins, raised shoulders, or collapsed centers are interpreted to indicate permafrost processes analogous with those occurring in polar terrains on Earth (morphologies produced by differential sublimation and winnowing of overlying sediments, thermal expansion against wedge materials, and ice loss, respectively) [Lachenbruch, 1962; Washburn, 1973; French, 1976; Marchant et al., 2002; Marchant and Head, 2007].

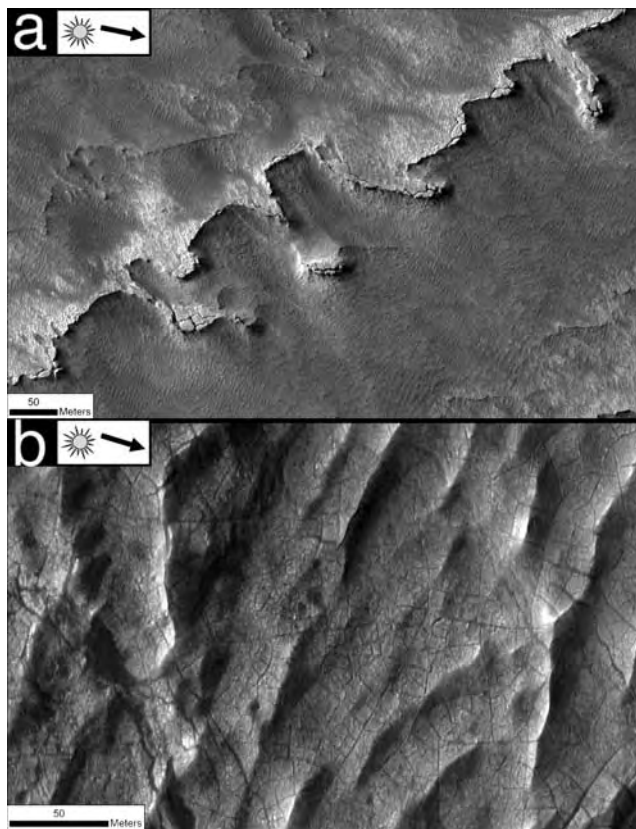


**Figure A1.** (a) Polygonal fractures interpreted to arise from processes other than thermal contraction cracking of ice-rich permafrost. The prevalence of fractures at the steep margin of a layered bedrock outcrop, coupled with the outcrop's high albedo, and lack of multiple generations of cracks suggests that bedrock jointing may better account for the polygonal fractures observed. Illumination is from the left. Portion of HiRISE image PSP\_003934\_1275, located east of the Argyre Basin. (b) Polygonal fractures in proximity to chloride-bearing units [Osterloo et al., 2008] on Arsia Mons. The presence of fractures that are entirely insensitive to local topography, coupled with a high albedo, and location in a bounded depression, suggests that these fractures may result from desiccation associated with salt presence [Osterloo et al., 2008]. Illumination is from the left. Portion of HiRISE image PSP\_003160\_1410.

Upturned edges typical of mud desiccation cracks [e.g., Heldmann et al., 2008] have not been observed at HiRISE resolution.

#### A1.3. Diameter/Size

[49] Tectonic or structural fractures can extend for multiple kilometers [Hiesinger and Head, 2000; Okubo and McEwen, 2007]. Thermal contraction cracks commonly form polygonal networks with polygon spacing of meters to ten of meters [Lachenbruch, 1962; Washburn, 1973; Pewe, 1974; Black, 1982; Plug and Werner, 2001]. Fractures interpreted to be desiccation cracks occur at scales  $< 50$  m, but can be highly variable in size and organization [Osterloo et al., 2008]. This analysis focuses on polygons with diameters generally  $< \sim 25$ , although throughgoing fractures are present in some HiRISE images which may extend for hundreds of meters.

#### A1.4. Latitude

[50] Features interpreted to be active thermal contraction crack polygons are present primarily in latitudes poleward of 30°. This latitude distribution is consistent with models predicting the distribution of sufficient ground ice to cement permafrost [Mellon and Jakosky, 1995; Mellon et al., 2004], as well as models predicting the distribution of seasonal thermal stresses sufficient to generate thermal contraction cracking [Mellon, 1997]. This latitude distribution is consistent with measured concentrations of ground ice in the upper meter of the Martian surface as determined by gamma ray and neutron spectrometer measurements [Boynton et al., 2002; Feldman et al., 2002; Kuzmin et al., 2004; Mangold et al., 2004; Mitrofanov et al., 2007], as well as with infrared surface temperature detection of shallow ground ice [Bandfield, 2007; Bandfield and Feldman, 2008].

#### A1.5. Surface Topography and Slope Orientation

[51] Polygons interpreted to be desiccation cracks are found primarily in closed basins, including crater bottoms [Ehlmann et al., 2008; Osterloo et al., 2008] (Figure A1). Polygons interpreted to be thermal contraction cracks occur on all surfaces, including flat-lying plains, slopes, and enclosed basins [Mangold, 2005]. Polygons interpreted to be thermal contraction cracks are found in isolated groups on pole-facing slopes at low latitudes, consistent with orientation-dependent ice preservation [e.g., Hecht, 2002]. Other polygon-forming processes (e.g., jointing) are not strongly orientation dependent.

#### A1.6. Age of Host Geological Surface

[52] Small-scale polygons mapped at HiRISE and MOC resolution [e.g., Mangold, 2005; Levy et al., 2008b] are found primarily on young geological surfaces, particularly Amazonian terrains [Tanaka et al., 2005], and are strongly associated with young, latitude-dependent mantle surfaces [Mustard et al., 2001; Kreslavsky and Head, 2002; Head et al., 2003]. Fractures in surfaces interpreted to be desiccated salt deposits are predominantly found on unmantled Hesperian and Noachian surfaces [Ehlmann et al., 2008; Osterloo et al., 2008].

#### A1.7. Particle Size

[53] On Mars, fractures interpreted to be thermal contraction cracks occur in surface sediments ranging in size from subpixel (<25 cm) to multimeter. Boulders present in thermal contraction crack polygon terrains are commonly distributed preferentially in polygon centers or at the base of polygon troughs [Mellon et al., 2007, 2008]. In contrast, desiccation-cracked units are commonly free of large particles detectible in HiRISE images [Fassett et al., 2007; Schon et al., 2008a].

#### A1.8. Bedrock Presence

[54] Polygons interpreted to be thermal contraction crack features are present in continuous and dissected mantle units that blanket underlying topography [e.g., Mustard et al., 2001; Kreslavsky and Head, 2002; Head et al., 2003]. Joint-induced fracture networks are commonly present in bedrock outcrops with significant topographic relief (e.g., butte tops, mesas) and visible layering. Fractures produced by thermal contraction of cooling melt are present in crater interiors [e.g., Milazzo et al., 2008] and in lava flows.

#### A1.9. Associated Landforms

[55] Polygons interpreted to result from desiccation in playa-like environments commonly occur in basins interpreted to be paleolakes, as indicated by basin topography, breaching fluvial channels, and/or sedimentary fans [e.g., Ehlmann et al., 2008; Fassett and Head, 2008b; Osterloo et al., 2008]. Thermal contraction crack polygons occur in many environments lacking fluvial landforms, although features interpreted to be thermal contraction crack polygons are present in some gullied terrains [e.g., Levy et al., 2008a, 2009b].

#### A1.10. Albedo

[56] Desiccation cracks are present primarily in high-albedo, light-toned deposits, commonly composed of phyllosilicates [Ehlmann et al., 2008] and/or salts [Osterloo et al., 2008]. Thermal contraction crack polygons form in units with moderate to low albedo (although seasonal, high-albedo frost can obscure underlying polygons) [Christensen et al., 2001].

#### A2. Factors Compromising Polygon Classification

[57] Identification and classification of polygonally patterned ground was hampered in some images by a variety of effects. Images acquired during winter conditions commonly have thick surface frost coatings (up to 10s of cm in some images) [Smith et al., 2001; Feldman et al., 2003], which can partially, or completely obscure polygonal patterning. This seasonal variability in image quality accounts for the relatively low number of southern hemisphere images in low orbit numbers, and the decreasing number of northern hemisphere images in high orbit numbers in this survey. Clouds are present in some images, obscuring portions of the surface, limiting polygon classification. Finally, regional and global dust storm conditions completely prevent the observation of surface features including polygons in some images.

[58] **Acknowledgments.** We gratefully acknowledge financial assistance from the NASA Mars Data Analysis Program grants NNG04GJ99G and NNX07AN95G, the NASA Mars Fundamental Research Program grant GC196412NGA, and the NASA Applied Information Systems Research Program grant NNG05GA61G. Special thanks to Caleb Fassett for assistance in processing and interpreting crater count information. Thanks also to James Dickson for coordination of image processing.

#### References

- Arvidson, R., et al. (2008), Mars exploration program 2007 Phoenix landing site selection and characteristics, *J. Geophys. Res.*, *113*, E00A03, doi:10.1029/2007JE003021.
- Bandfield, J. L. (2007), High-resolution subsurface water-ice distributions on Mars, *Nature*, *447*(7140), 64–67, doi:10.1038/nature05781.
- Bandfield, J. L., and W. C. Feldman (2008), Martian high latitude permafrost depth and surface cover thermal inertia distributions, *J. Geophys. Res.*, *113*, E08001, doi:10.1029/2007JE003007.
- Berg, T. E., and R. F. Black (1966), Preliminary measurements of growth of nonsorted polygons, Victoria Land, Antarctica, in *Antarctic Soils and Soil-Forming Processes*, *Antarct. Res. Ser.*, vol. 8, edited by J. C. F. Tedrow, pp. 61–108, AGU, Washington, D. C.
- Black, R. F. (1952), Polygonal patterns and ground conditions from aerial photographs, *Photogramm. Eng.*, *17*, 123–134.
- Black, R. F. (1982), Patterned-ground studies in Victoria Land, *Antarct. J. U.S.*, *17*(5), 53–54.
- Boynton, W. V., et al. (2002), Distribution of hydrogen in the near-surface of Mars: Evidence for sub-surface ice deposits, *Science*, *297*, 81–85, doi:10.1126/science.1073722.
- Buczkowski, D. L., and M. L. Cooke (2004), Formation of double-ring circular grabens due to volumetric compaction of over buried impact craters: Implications for thickness and nature of cover material in Utopia Planitia, Mars, *J. Geophys. Res.*, *109*, E02006, doi:10.1029/2003JE002144.

- Christensen, P. R., et al. (2001), Mars Global Surveyor Thermal Emission Spectrometer experiment: Investigation description and surface science results, *J. Geophys. Res.*, *106*(E10), 23,823–23,872.
- Costard, F., F. Forget, J.-B. Madeleine, R. J. Soare, and J. S. Kargel (2008), The origin and formation of scalloped terrain in Utopia Planitia: Insight from a general circulation model, *Lunar Planet. Sci.*, *XXXIX*, abstract 1274.
- Dobrea, E. Z. N., E. Asphaug, J. A. Grant, M. A. Kessler, and M. T. Mellon (2007), Patterned ground as an alternative explanation for the formation of brain coral textures in the mid latitudes of Mars: HiRISE observations of lineated valley fill textures, paper presented at 7th International Conference on Mars, Lunar and Planet. Inst., Pasadena, Calif, 9–13 July.
- Ehlmann, B. L., J. F. Mustard, C. I. Fassett, S. C. Schon, J. W. Head, D. J. Des Marais, J. A. Grant, and S. L. Murchie (2008), Clay minerals in delta deposits and organic preservation potential on Mars, *Nat. Geosci.*, *1*, 355–358, doi:10.1038/ngeo207.
- Fassett, C. I., and J. W. Head (2008a), The timing of Martian valley network activity: Constraints from buffered crater counting, *Icarus*, *195*, 61–89.
- Fassett, C. I., and J. W. Head (2008b), Open-basin lakes on Mars: Implications of valley network lakes for the nature of Noachian hydrology, *Lunar Planet. Sci.*, *XXXIX*, abstract 1139.
- Fassett, C. I., B. L. Ehlmann, J. W. Head, J. F. Mustard, S. C. Schon, and S. L. Murchie (2007), Sedimentary fan deposits in Jezero Crater Lake, in the Nili Fossae region, Mars: Meter-scale layering and phyllosilicate-bearing sediments, *Eos Trans. AGU*, *88*(52), Fall Meet. Suppl., Abstract P13D-1562.
- Feldman, W. C., et al. (2002), Global distribution of neutrons from Mars: Results from Mars Odyssey, *Science*, *297*, 75–78, doi:10.1126/science.1073541.
- Feldman, W. C., et al. (2003), CO<sub>2</sub> frost cap thickness of Mars during northern winter and spring, *J. Geophys. Res.*, *108*(E9), 5103, doi:10.1029/2003JE002101.
- Feldman, W. C., J. L. Bandfield, B. Diez, R. C. Elphic, S. Maurice, and S. M. Nelli (2008), North to south asymmetries in the water-equivalent hydrogen distribution at high latitudes on Mars, *J. Geophys. Res.*, *113*, E08006, doi:10.1029/2007JE003020.
- French, H. M. (1976), *The Periglacial Environment*, 309 pp., Longman, London.
- Ghysels, G., and I. Heyse (2006), Composite-wedge pseudomorphs in Flanders, Belgium, *Permafrost Periglacial Processes*, *17*, 145–161, doi:10.1002/ppp.552.
- Grotzinger, J., et al. (2006), Sedimentary textures formed by aqueous processes, Erebus crater, Meridiani Planum, Mars, *Geology*, *34*(12), 1085–1088, doi:10.1130/G22985A.1.
- Hartmann, W. K. (2005), Martian cratering 8: Isochron refinement and the chronology of Mars, *Icarus*, *174*(2), 294–320, doi:10.1016/j.icarus.2004.11.023.
- Hartmann, W. K. (2008), Age of Gratteri crater: Preliminary test of the crater-count isochron chronometric systems, *Lunar Planet. Sci.*, *XXXIX*, abstract 1844.
- Hartmann, W. K., G. Neukum, and S. Werner (2008), Confirmation and utilization of the “production function” size-frequency distributions of Martian impact craters, *Geophys. Res. Lett.*, *35*, L02205, doi:10.1029/2007GL031557.
- Head, J. W., J. F. Mustard, M. A. Kreslavsky, R. E. Milliken, and D. R. Marchant (2003), Recent ice ages on Mars, *Nature*, *426*(6968), 797–802, doi:10.1038/nature02114.
- Head, J. W., D. R. Marchant, and M. A. Kreslavsky (2008), Formation of gullies on Mars: Link to recent climate history and insolation microenvironments implicate surface water flow origin, *Proc. Natl. Acad. Sci. U. S. A.*, *105*, 13,258–13,263, doi:10.1073/pnas.0803760105.
- Hecht, M. H. (2002), Metastability of water on Mars, *Icarus*, *156*, 373–386, doi:10.1006/icar.2001.6794.
- Heldmann, J. L., C. Conley, A. J. Brown, L. Fletcher, J. L. Bishop, and C. P. McKay (2008), Atacama desert mudflow as an analog for recent gully activity on Mars, *Lunar Planet. Sci.*, *XXXIX*, abstract 2214.
- Hiesinger, H., and J. W. Head (2000), Characteristics and origin of polygonally terrain in southern Utopia Planitia, Mars: Results from Mars Orbiter Laser Altimeter and Mars Orbiter Camera data, *J. Geophys. Res.*, *105*(E05), 11,999–12,022.
- Ivanov, B. A., et al. (2008), Small impact crater clusters in high resolution HiRISE images, *Lunar Planet. Sci.*, *XXXIX*, abstract 1221.
- Kanner, L. C., C. C. Allen, and M. S. Bell (2004), Geomorphic evidence for Martian ground ice and climate change, *Lunar Planet. Sci.*, *XXXV*, abstract 1982.
- Kostama, V.-P., M. A. Kreslavsky, and J. W. Head (2006), Recent high-latitude icy mantle in the northern plains of Mars: Characteristics and ages of emplacement, *Geophys. Res. Lett.*, *33*, L11201, doi:10.1029/2006GL025946.
- Kowalewski, D. E., D. R. Marchant, J. S. Levy, and J. W. Head (2006), Quantifying summertime sublimation rates for buried glacier ice in Beacon Valley, Antarctica, *Antarct. Sci.*, *18*(3), 421–428, doi:10.1017/S0954102006000460.
- Kreslavsky, M. (2008), Young populations of small craters on Mars: A case study, paper presented at 3rd European Planetary Science Congress, Europlanet, Munster, Germany, 22–25 Sept.
- Kreslavsky, M., and J. Head (1999), Kilometer-scale slopes on Mars and their correlation with geologic units: Initial results from Mars Orbiter Laser Altimeter (MOLA) data, *J. Geophys. Res.*, *104*(E9), 21,911–21,924, doi:10.1029/1999JE001051.
- Kreslavsky, M. A., and J. W. Head (2002), Mars: Nature and evolution of young, latitude-dependent water-ice-rich mantle, *Geophys. Res. Lett.*, *29*(15), 1719, doi:10.1029/2002GL015392.
- Kreslavsky, M. A., J. W. Head, and D. R. Marchant (2008), Periods of active permafrost layer formation during the geological history of Mars: Implications for circum-polar and mid-latitude surface processes, *Planet. Space Sci.*, *56*, doi:10.1016/j.pss.2006.02.010.
- Kuzmin, R. O., E. V. Zabalueva, I. G. Mitrofanov, M. L. Litvak, W. V. Boynton, and R. S. Saunders (2004), Regions of potential existence of free water (ice) in the near-surface Martian ground: Results from the Mars Odyssey High-Energy Neutron Detector (HEND), *Sol. Syst. Res.*, *38*(1), 1–11, doi:10.1023/B:SOLS.0000015150.61420.5b.
- Lachenbruch, A. H. (1961), Depth and spacing of tension cracks, *J. Geophys. Res.*, *66*(12), 4273–4292, doi:10.1029/JZ066i012p04273.
- Lachenbruch, A. H. (1962), Mechanics of thermal contraction cracks and ice-wedge polygons in permafrost, *Spec. Pap. Geol. Soc. Am.*, *70*, 1–69.
- Lefort, A., et al. (2007), Scalloped terrains in Utopia Planitia: Insight from HiRISE, *Lunar Planet. Sci.*, *XXXVIII*, abstract 1796.
- Levy, J. S., D. R. Marchant, and J. W. Head (2006), Distribution and origin of patterned ground on Mullins Valley debris-covered glacier, Antarctica: The roles of ice flow and sublimation, *Antarct. Sci.*, *18*(3), 385–397, doi:10.1017/S0954102006000435.
- Levy, J. S., J. W. Head, and D. R. Marchant (2008a), The role of thermal contraction crack polygons in cold-desert fluvial systems, *Antarct. Sci.*, *20*, 565–579, doi:10.1017/S0954102008001375.
- Levy, J. S., J. W. Head, D. R. Marchant, and D. E. Kowalewski (2008b), Identification of sublimation-type thermal contraction crack polygons at the proposed NASA Phoenix landing site: Implications for substrate properties and climate-driven morphological evolution, *Geophys. Res. Lett.*, *35*, L04202, doi:10.1029/2007GL032813.
- Levy, J. S., J. W. Head, and D. R. Marchant (2009a), Concentric crater fill in Utopia Planitia: Timing and transitions between glacial and periglacial processes, *Icarus*, in press.
- Levy, J. S., J. W. Head, D. R. Marchant, J. L. Dickson, and G. A. Morgan (2009b), Geologically recent gully polygon relationships on Mars: Insights from the Antarctic Dry Valleys on the roles of permafrost, microclimates, and water sources for surface flow, *Icarus*, in press.
- Lucchitta, B. K. (1981), Mars and Earth: Comparison of cold-climate features, *Icarus*, *45*, 264–303, doi:10.1016/0019-1035(81)90035-X.
- Malin, M. C., and K. S. Edgett (2001), Mars Global Surveyor Mars Orbiter Camera: Interplanetary cruise through primary mission, *J. Geophys. Res.*, *106*(E10), 23,429–423,540.
- Malin, M. C., K. S. Edgett, L. V. Posiolova, S. M. McColley, and E. Z. N. Dobrea (2006), Present-day impact cratering rate and contemporary gully activity on Mars, *Science*, *314*, 1573–1577, doi:10.1126/science.1135156.
- Malooof, A. C., J. B. Kellogg, and A. M. Anders (2002), Neoproterozoic sand wedges: Crack formation in frozen soils under diurnal forcing during a snowball Earth, *Earth Planet. Sci. Lett.*, *204*, 1–15, doi:10.1016/S0012-821X(02)00960-3.
- Mangold, N. (2005), High latitude patterned grounds on Mars: Classification, distribution and climatic control, *Icarus*, *174*, 336–359, doi:10.1016/j.icarus.2004.07.030.
- Mangold, N., S. Maurice, W. C. Feldman, F. Costard, and F. Forget (2004), Spatial relationships between patterned ground and ground ice detected by the Neutron Spectrometer on Mars, *J. Geophys. Res.*, *109*, E08001, doi:10.1029/2004JE002235.
- Marchant, D. R., and G. H. Denton (1996), Miocene and Pliocene paleoclimate on the Dry Valleys region, southern Victoria Land: A geomorphological approach, *Mar. Micropaleontol.*, *27*, 253–271, doi:10.1016/0377-8398(95)00065-8.
- Marchant, D. R., and J. W. Head (2007), Antarctic Dry Valleys: Microclimate zonation, variable geomorphic processes, and implications for assessing climate change on Mars, *Icarus*, *192*(1), 187–222, doi:10.1016/j.icarus.2007.06.018.
- Marchant, D. R., A. R. Lewis, W. M. Phillips, E. J. Moore, R. A. Souchez, G. H. Denton, D. E. Sugden, N. Potter Jr., and G. P. Landis (2002), Formation of patterned ground and sublimation till over Miocene glacier ice in Beacon Valley, southern Victoria Land, Antarctica, *Geol. Soc. Am. Bull.*,

- 114(6), 718–730, doi:10.1130/0016-7606(2002)114<0718:FOPGAS>2.0.CO;2.
- McBride, S. A., C. C. Allen, and M. S. Bell (2005), Prospecting for Martian ice, *Lunar Planet. Sci.*, XXXVI, abstract 1090.
- McEwen, A. S., et al. (2007), Mars Reconnaissance Orbiters High Resolution Imaging Science Experiment (HiRISE), *J. Geophys. Res.*, 112, E05S02, doi:10.1029/2005JE002605.
- Mellon, M. T. (1997), Small-scale polygonal features on Mars: Seasonal thermal contraction cracks in permafrost, *J. Geophys. Res.*, 102(E11), 25,617–625, doi:10.1029/97JE02582.
- Mellon, M. T., and B. M. Jakosky (1995), The distribution and behavior of Martian ground ice during past and recent epochs, *J. Geophys. Res.*, 100(E6), 11,781–711,799.
- Mellon, M. T., W. C. Feldman, and T. H. Prettyman (2004), The presence and stability of ground ice in the southern hemisphere of Mars, *Icarus*, 169(2), 324–340, doi:10.1016/j.icarus.2003.10.022.
- Mellon, M. T., et al. (2007), HiRISE observations of patterned ground on Mars, paper presented at 7th International Conference on Mars, Lunar and Planet. Inst., Pasadena, Calif., 9–13 July.
- Mellon, M. T., R. E. Arvidson, J. J. Marlow, R. J. Phillips, and E. Asphaug (2008), Periglacial landforms at the Phoenix landing site and the northern plains of Mars, *J. Geophys. Res.*, 113, E00A23, doi:10.1029/2007JE003039.
- Milazzo, M. P., W. L. Jaeger, L. Keszthelyi, A. S. McEwen, and R. A. Beyer (2008), The discovery of columnar jointing on Mars, *Lunar Planet. Sci.*, XXXIX, abstract 2062.
- Milliken, R. E., J. F. Mustard, and D. L. Goldsby (2003), Viscous flow features on the surface of Mars: Observations from high-resolution Mars Orbiter Camera (MOC) images, *J. Geophys. Res.*, 108(E6), 5057, doi:10.1029/2002JE002005.
- Mitrofanov, I. G., M. T. Zuber, M. L. Litvak, N. E. Demidov, A. B. Sanin, and W. V. Boynton (2007), Burial depth of water ice in Mars permafrost subsurface, *Lunar Planet. Sci.*, XXXVIII, abstract 3108.
- Morgan, G. A., J. W. Head, D. R. Marchant, J. L. Dickson, and J. S. Levy (2007), Gully formation on Mars: Testing the snowpack hypothesis from analysis of analogs in the Antarctic Dry Valleys, *Lunar Planet. Sci.*, XXXVIII, abstract 1656.
- Morgenstern, A., E. Hauber, D. Reiss, S. van Gasselt, G. Grosse, and L. Schirmer (2007), Deposition and degradation of a volatile-rich layer in Utopia Planitia and implications for climate history on Mars, *J. Geophys. Res.*, 112, E06010, doi:10.1029/2006JE002869.
- Murton, J. B., P. Worsley, and J. Gozdzik (2000), Sand veins and wedges in cold aeolian environments, *Quat. Sci. Rev.*, 19, 899–922, doi:10.1016/S0277-3791(99)00045-1.
- Mustard, J. F., C. D. Cooper, and M. K. Rifkin (2001), Evidence for recent climate change on Mars from the identification of youthful near-surface ground ice, *Nature*, 412(6845), 411–414, doi:10.1038/35086515.
- Mutch, T. A., et al. (1976), The surface of Mars: The view from the Viking 2 Lander, *Science*, 194(4271), 1277–1283, doi:10.1126/science.194.4271.1277.
- Mutch, T. A., R. E. Arvidson, E. A. Guinness, A. B. Binder, and E. C. Morris (1977), The geology of the Viking Lander 2 site, *J. Geophys. Res.*, 82, 4452–4467, doi:10.1029/JS082i028p04452.
- Neal, J. T., A. M. Langer, and P. F. Kerr (1968), Giant desiccation polygons of Great Basin playas, *Geol. Soc. Am. Bull.*, 79, 69–90, doi:10.1130/0016-7606(1968)79[69:GDPOGB]2.0.CO;2.
- Neukum, G., and B. A. Ivanov (2001), Crater production functions for Mars, *Lunar Planet. Sci.*, XXXII, abstract 1757.
- Okubo, C. H., and A. S. McEwen (2007), Fracture-controlled paleo-fluid flow in Candor Chasma, Mars, *Science*, 315(5814), 983–985, doi:10.1126/science.1136855.
- Osterloo, M. M., V. E. Hamilton, J. L. Bandfield, T. D. Glotch, A. M. Baldridge, P. R. Christensen, L. L. Tornabene, and F. S. Anderson (2008), Chloride-bearing materials in the southern highlands of Mars, *Science*, 319, 1651–1654, doi:10.1126/science.1150690.
- Pewe, T. L. (1959), Sand-wedge polygons (tessellations) in the McMurdo Sound region, Antarctica-A progress report, *Am. J. Sci.*, 257, 545–552.
- Pewe, T. L. (1963), Ice-wedges in Alaska-classification, distribution, and climatic significance, paper presented at 2nd International Conference on Permafrost, Russ. Acad. of Sci., Yakutsk, Siberia.
- Pewe, T. L. (1974), Geomorphic processes in polar deserts, in *Polar Deserts and Modern Man*, edited by T. L. Smiley and J. H. Zumberge, pp. 33–52, Univ. of Ariz. Press, Tucson.
- Plug, L. J., and B. T. Werner (2001), Fracture networks in frozen ground, *J. Geophys. Res.*, 106(B5), 8599–8613, doi:10.1029/2000JB900320.
- Reiss, D., S. van Gasselt, G. Neukum, and R. Jaumann (2004), Absolute dune ages and implications for the time of formation of gullies in Nirgal Vallis, Mars, *J. Geophys. Res.*, 109, E06007, doi:10.1029/2004JE002251.
- Root, J. D. (1975), *Ice-Wedge Polygons, Tuktoyaktuk Area, North–West Territories*, 181 pp., Geol. Surv. of Can, Ottawa, Ont.
- Schon, S. C., C. I. Fassett, and J. W. Head (2008a), Meander loops and point bar sequences: Evidence of a stable delta plain environment in Jezero crater, *Lunar Planet. Sci.*, XXXIX, abstract 1354.
- Schon, S. C., J. W. Head, and C. I. Fassett (2008b), Unique chronostratigraphic maker in depositional fan stratigraphy on Mars: Evidence for ~1.25 Ma old gully activity and surficial meltwater origin, *Geology*, in press.
- Schorghofer, N. (2007), Dynamics of ice ages on Mars, *Nature*, 449(7159), 192–194, doi:10.1038/nature06082.
- Schorghofer, N., and O. Aharonson (2005), Stability and exchange of sub-surface ice on Mars, *J. Geophys. Res.*, 110, E05003, doi:10.1029/2004JE002350.
- Seibert, N. M., and J. S. Kargel (2001), Small-scale Martian polygonal terrain: Implications for liquid surface water, *Geophys. Res. Lett.*, 28(5), 899–902, doi:10.1029/2000GL012093.
- Skinner, J. A., Jr., T. M. Hare, and K. L. Tanaka (2006), Digital renovation of the atlas of Mars: 1:15000000-scale global geologic series maps, *Lunar Planet. Sci.*, XXXVII, abstract 2331.
- Sletten, R. S., B. Hallet, and R. C. Fletcher (2003), Resurfacing time of terrestrial surfaces by the formation and maturation of polygonally patterned ground, *J. Geophys. Res.*, 108(E4), 8044, doi:10.1029/2002JE001914.
- Smith, D. E., M. T. Zuber, and G. A. Neumann (2001), Seasonal variations of snow depth on Mars, *Science*, 294(5549), 2141–2146, doi:10.1126/science.1066556.
- Smith, P. H. (2008), Phoenix on Mars: The prime mission, *Bull. Am. Astron. Soc.*, 40, 56.02.
- Smith, P. H., et al. (2007), The Phoenix Mission, paper presented at 7th International Conference on Mars, Lunar and Planet. Inst., Pasadena, Calif., 9–13 July.
- Soare, R. J., G. R. Osinski, and C. L. Roehm (2008), Thermokarst lakes and ponds on Mars in the very recent (late Amazonian) past, *Earth Planet. Sci. Lett.*, 272(1–2), 382–393, doi:10.1016/j.epsl.2008.05.010.
- Tanaka, K. L., et al. (2005), Geologic map of the northern plains of Mars, U.S. Geol. Surv. Sci. Invest. Map, 2888.
- Washburn, A. L. (1973), *Periglacial Processes and Environments*, 320 pp., St. Martins Press, New York.
- Yershov, E. D. (1998), *General Geocryology*, 580 pp., Cambridge Univ. Press, Cambridge, U. K.
- Zanetti, M., H. Hiesinger, D. Reiss, E. Hauber, and G. Neukum (2008), Scalloped depressions in Malea Planum, southern Hellas Basin, Mars, *Lunar Planet. Sci.*, XXXIX, abstract 1682.

J. Head and J. Levy, Department of Geological Sciences, Brown University, 324 Brook Street, Box 1846, Providence, RI 02912, USA. (joseph\_levy@brown.edu)

D. Marchant, Department of Earth Sciences, Boston University, 675 Commonwealth Avenue, Boston, MA 02215, USA.